EPDM/PP Thermoplastic Vulcanizates As Studied by Proton NMR Relaxation: Phase Composition, Molecular Mobility, Network Structure in the Rubbery Phase, and Network Heterogeneity

V. M. Litvinov

DSM Research, Resolve, P.O. Box 18, 6160 MD Geleen, The Netherlands

Received August 18, 2006; Revised Manuscript Received September 28, 2006

ABSTRACT: Proton solid-state NMR T_2 relaxation analysis is used to study model oil-extended ethylene−propylene-diene rubber (EPDM) and thermoplastic vulcanizates (TPV) composed of polypropylene (PP), EPDM and oil. It is shown that the method allows selective characterization of crystalline and amorphous phases of PP, cross-linked EPDM, and oil in TPVs. The network density in the rubbery (EPDM) phase is determined in a wide range of the TPV compositions, as well as in the oil-extended EPDM vulcanizates containing different amount of oil. The entanglement density decreases with increasing oil content in oil-extended EPDM. This decrease can be described using a scaling approach. Molecular mobility of oil molecules decreases with increasing EPDM network density and is significantly lower than that of pure oil due to physical interactions with the host matrix. It is shown that the network density in the rubbery phase of TPV is composed of chemical cross-links, physical junctions at the EPDM/PP interface, and temporary and trapped chain entanglements. The density of chemical cross-links increases with the amount of cross-linker per weight unit of EPDM. The density of the physical junctions increases with increasing PP content. Crystallinity of PP in TPV is hardly affected by the TPV composition. A small fraction of oil molecules plasticizes the amorphous phase of PP and the plasticization effect is proportional to an oil:PP mass ratio in the TPV composition. Two NMR methods for improving the selectivity of the T_2 relaxation analysis to different phases of TPV are evaluated. The methods are based on the inversion−recovery experiment and double-quantum (DQ) filtering of the decay of the transverse magnetization relaxation. The DQ filtered T_2 relaxation experiment improves the selectivity of the method and could open new possibilities for characterization of the network heterogeneity in rubbery materials. Some relationships between the TPV composition, network density, and mechanical properties are shortly discussed.

1. Introduction

Thermoplastic elastomers (TPE) are rubbery materials that are processable as thermoplastics but exhibit properties similar to those of vulcanized rubbers at usage temperatures.[1−3] Thermoplastic vulcanizates (TPV) are an important class of TPEs that are produced by dynamic vulcanization of blends containing a thermoplastic and an elastomer. Commercial TPVs are often made from isotactic polypropylene (PP), ethylene−propylene−diene rubber (EPDM) and extender oil.[2,4] The addition of oil in combination with cross-linking of the EPDM allows one to produce soft compositions with good processability and elastic recovery. During dynamic vulcanization, the rubber is vulcanized in the presence of the molten thermoplastic under shear forces. Since cross-linked rubber is unable to coalesce, rubber particles are dispersed in the thermoplastic matrix even at high rubber content.[1,2,5] The size of the rubbery particles is affected by the composition of TPVs and processing conditions and is in the range of one to few micrometers.[1,2,6] The dispersed EPDM phase may contain occluded PP particles.[7] TPVs show fairly good elastic behavior because both the rubber particles and the thin PP layers surrounding the particles behave elastically upon deformation.[8,9]

Knowledge of the physical state of oil in TPVs is of large importance for understanding the elastic properties of these materials. It has been shown that oil is mixed on a molecular scale with PP and EPDM in their binary blends, as well as in EPDM/PP TPVs.[6] The oil resides both in the thermoplastic continuous phase and in the EPDM phase because of a small difference in the polarity of the olefinic oil, PP and EPDM. Oil molecules plasticize the amorphous phase of PP,[10−12] and reduce the entanglement density in the rubbery phase.[13] Different methods have been used for determining the partitioning of oil molecules between the EPDM and PP phases in TPVs: the depression of T_g measured by dynamic mechanical thermal analysis (DMTA),[10] differential scanning calorimetry (DSC)[14] and dielectric spectroscopy (DIES).[14] The oil distribution in TPVs has also been studied by the integration of the surface area of TEM images,[15] and by ^{13}C solid-state NMR spectroscopy.[16] However, all these methods suffer from a lack of accuracy.

Another important molecular characteristic of TPVs is the network density in the rubbery phase. Despite several methods that have been evaluated for determining the network density in the rubbery phase of TPVs, none of these methods has provided accurate quantitative information on the network structure. The following methods have been proposed for determining the relative differences in the network density in a series of TPVs samples: equilibrium swelling,[2] the elastic storage modulus,[17] force modulated atomic force microscopy (AFM),[12] determining molecular mobility of dissolved in the rubbery phase probe molecules using electron spin resonance (ESR),[18] the analysis of unreacted phenolic groups of cross-linker (phenolic resin) and unreacted diene of EPDM using high-resolution proton solid-state NMR spectroscopy,[12] determining the line broadening in the proton NMR spectra,[12] and the analysis of $^1H-^{13}C$ polarization transfer dynamics in ^{13}C CPMAS solid-state NMR experiment.[19]

In this work, low-field proton NMR T_2 relaxation experiments will be used for studying (1) the network density in the rubbery phase of EPDM/PP TPVs, (2) the phase composition of TPVs, (3) molecular mobility of oil molecules, and (4) the effect of

10.1021/ma061911h CCC: $33.50
Published on Web 11/11/2006

Table 1. Composition of Oil-Extended EPDM Sulfur Vulcanizates in Weight Parts per 100 Weight Parts of EPDM (phr)[a]

	EPDM/0	EPDM/4	EPDM/8	EPDM/12	EPDM/30	EPDM/50	EPDM/100
EPDM	100	100	100	100	100	100	100
Sunpar 2280	0	4	8	12	30	50	100
ZnO	5	5	5	5	5	5	5
stearic acid	1	1	1	1	1	1	1
MBT-80	0.63	0.63	0.63	0.63	0.63	0.63	0.63
TMTD-80	1.25	1.25	1.25	1.25	1.25	1.25	1.25
sulfur S-80	1.88	1.88	1.88	1.88	1.88	1.88	1.88

[a] The samples are identified by a code such as EPDM/4 that indicates the amount of oil. MBT and TMDT stand for mercaptobenzothiazole and tetramethylthiuram disulfide.

oil on the molecular mobility in the EPDM and PP phases. It was shown previously that the method provides quantitative data on the phase composition of random polypropylene copolymers,[20] the density of chemical cross-links, and chain entanglements in EPDM rubbers[13,21,22] and offers high selectivity for quantitative analysis of the network density in rubber-toughened thermoplastics.[23] A series of model TPVs with a wide range of the composition was prepared for this study. Some mechanical properties of the TPVs will be discussed in relation to the molecular characteristics that are determined for the samples by the NMR method.

2. Experimental Section

2.1. Samples. Two series of samples were studied: (1) oil-extended EPDM, vulcanizates thereof and residual gel after extraction of oil from the vulcanizates; (2) thermoplastic EPDM/PP dynamic vulcanizates.

Oil-extended EPDM samples were prepared by mixing with a kneader EPDM rubber with different amounts of paraffinic oil Sunpar 2280. Sunpar oil is a complex mixture of hydrocarbons with a relatively broad molar mass distribution. The EPDM rubber was composed of 44.6 wt % ethylene, 45.4 wt % propylene, and 10 wt % 5-ethylidene-2-norbornene (ENB). Molecular weight characteristics of the EPDM were the following: $M_n = 44$ g/mol, $M_w = 172$ g/mol, and $M_z = 484$ g/mol. Sunpar 2280 was composed of 67 wt % paraffinic, 29 wt % naphthenics, and 4 wt % aromatic fractions. Sulfur vulcanization of the oil-extended EPDM was performed in 2 mm press plates at 175 °C. The sample compositions and the vulcanization recipe are given in Table 1. The vulcanizates were studied as a whole and as residual gel. Oil in the vulcanizates was extracted in boiling pentanon-3. After the extraction, the rubber gel was dried in an oven at 70 °C in a vacuum of 170 mmHg under a flow of nitrogen, until the sample weight remained constant in time. Hardly any unvulcanized EPDM could be detected in the sol fraction with IR spectroscopy.

TPVs were prepared on a laboratory scale by dynamic vulcanization of a mixture of EPDM rubber, isotactic PP homopolymer and extender oil Sunpar 2280. The material was cross-linked with (*p*-isooctylphenol)−formaldehyde resin (resol; Schenectady SP 1045) activated by stannous chloride and zinc oxide.[24] The EPDM rubber was composed of 64.6 wt % ethylene units, 28.2 wt % propylene units, 5.0 wt % ENB, and 2.2 wt % dicyclopentadiene. Molecular weight characteristics of the EPDM were the following: $M_n = 50$ g/mol, $M_w = 160$ g/mol, and $M_z = 500$ g/mol. The TPV sample compositions are given in Table 2.

Peroxide cured EPDM/PP TPVs were used for NMR experiments with inversion−recovery and DQ filter experiments. Details of sample preparation will be provided in an upcoming publication.[25] The sample compositions are given in figure captions.

2.2. Solid-State Proton NMR Measurements and Data Analysis. 2.2.1. Equipment. Proton NMR transverse magnetization relaxation (T_2 relaxation) experiments were performed on Bruker Minispec NMS-120 and MQ-20 spectrometers. These spectrometers operate at a proton resonance frequency of 20 MHz. The length of the 90° pulse and the dead time were 2.8 and 7 μs, respectively. A BVT-3000 temperature controller was used for temperature regulation. The temperature gradient within sample volume and stability had an accuracy better than 1 °C.

Table 2. Composition of Model TPVs (in wt %)[a]

TPV	1	2	3	4	5	6	7	8
PP	20.6	20.2	19.3	12.0	30.0	44.9	20.1	29.1
EPDM	55.6	55.6	55.6	46.8	57.1	50.3	76.7	68.1
Sunpar 2280	21.9	21.9	21.9	39.3	10.5	2.64		
PhR	0.44	0.88	1.75	0.74	0.90	0.79	1.21	1.07
TC	0.44	0.44	0.44	0.37	0.45	0.40	0.60	0.53
Zn0	0.53	0.53	0.53	0.44	0.54	0.48	0.72	0.64
Irganox 1076	0.46	0.46	0.46	0.39	0.48	0.42	0.66	0.57
PhR/EPDM	7.9	15.8	31.5	15.8	15.8	15.7	15.8	15.7
EPDM/PP	2.7	2.8	2.9	3.9	1.9	1.1	3.82	2.34

TPV	9	10	11	12	13	14	15
PP	46.3	80.0	19.3	20.2	12.0	30.0	44.9
EPDM	51.6	19.2	38.8	38.8	43.0	33.8	26.5
Sunpar 2280	-	-	38.7	38.7	43.1	33.8	26.5
PhR	0.81	0.30	1.75	0.88	0.74	0.90	0.79
TC	0.41	0.15	0.44	0.44	0.37	0.45	0.40
ZnO	0.48	0.18	0.53	0.53	0.44	0.54	0.48
Irganox 1076	0.44	0.16	0.48	0.46	0.39	0.48	0.42
PhR/EPDM	15.4	15.6	45.1	22.7	17.2	26.6	29.8
EPDM/PP	1.11	0.24	2.01	1.92	3.58	1.13	0.59

[a] PhR and TC stand for phenolic resin Schenectedy SP1045, and TC for tin chloride, respectively. PhR/EPDM is the weight ratio phenolic resin: EPDM, multiplied by 1000. EPDM/PP is the weight ratio EPDM: PP.

2.2.2. NMR Relaxation Experiments. Three different pulse sequences were used to record the decay of the transverse magnetization relaxation (T_2 decay) from rigid (crystalline), rubbery, and oil fractions of the TPVs. Accurate measurement of T_2 relaxation time and the amount of a rigid phase in the presence of a soft phase/component requires the following experiments:[20,26] (1) *a solid echo pulse sequence* (SEPS) and (2) the free induction decay (FID) after a *single pulse (usually 90°) pulse excitation* (SPE). Both methods could cause systematic errors in the analysis of the phase composition in heterogeneous materials. Because of the dead time of the receiver, the initial part of the FID is not detected after the 90° pulse excitation: [90°$_x$−the dead time−acquisition of the amplitude of the transverse magnetization A(t) as a function of time t after 90° pulse]. Therefore, the knowledge of the FID shape for the rigid fraction is required for accurate deconvolution of the FID into components corresponding to rigid and soft fractions. The shape of the FID for the rigid phase can be determined by the SEPS: [90°$_x$−t_{se}−90°$_y$−t_{se}−acquisition of the amplitude of the transverse magnetization $A(t)$], with t_{se} of 10 μs. The point in time from the beginning of the first pulse $t = (2t_{se} + t_{90})$ was taken as zero, where t_{90} was the duration of the 90° pulse. SEPS has the advantage of avoiding the dead time of NMR spectrometers. The solid-echo is formed with a maximum at approximately $t = (2t_{se} + t_{90})$. The SEPS allows accurate measurement of the shape of the initial part of the FID for the rigid fraction at short t_{se}. However, the rigid/soft ratio measured with SEPS for semicrystalline polymers above T_g can be somewhat lower than its true value,[20,26] because of the following reasons: (1) the incomplete refocusing of the dipolar interactions by the solid-echo for a dipolar network (see for instance ref 27), (2) molecular motions, the correlation time of which is comparable to the pulse spacing,[28] and (3) the shift of the echo maximum due to a nonzero pulse width.[29,30] The analysis of the FID, as recorded

using the SEPS, has shown that the FID shape for the rigid fraction of TPVs is close to Gaussian, similar to that for a random PP copolymer.[20] As far as the soft fraction of TPVs is concerned, the shape of the FID from this fraction is affected by heterogeneity of the permanent magnetic field B_o within the sample volume due to heterogeneity of B_o itself and its heterogeneity across the sample due to magnetic susceptibility differences between the soft and hard phases of TPVs. This does not allow using the SPE for characterization of the soft phase of TPVs.

A Hahn echo pulse sequence (HEPS), $90°_x - t_{He} - 180°_y - t_{He} -$ [acquisition of the amplitude of an echo maximum $A(t)$], was used to record the slow part of the T_2 relaxation decay for the soft fraction of the TPVs, where t_{He} was varied between 35 μs and 400 ms. At $t_{He} \geq 35$ μs, the major part of the signal from the rigid fraction decays nearly to zero. Therefore, the second pulse in the HEPS reverses nuclear spins of the soft fraction only, and an echo signal is formed with a maximum at time $t = (2t_{He} + t_{90/2} + t_{180/2})$ from the beginning of the first pulse, where $t_{180}/2$ is the half time of the 180° pulse. By varying the pulse spacing in the HEPS, the amplitude of the transverse magnetization $A(t)$ is measured as a function of time t. The HEPS makes it possible to eliminate the magnetic field and chemical shift inhomogeneities, and to accurately measure the T_2 relaxation time for the soft fractions/phases. It should be mentioned that the T_2 relaxation of oil, as determined by the HEPS, is affected by self-diffusion of oil molecules.

Thus, both the SPE and the HEPS experiments have to be used for determining the absolute value of the amount and T_2 values of the low mobile and mobile fractions in TPVs. The T_2 relaxation time and the amount of the rigid fraction were determined by analysis of the FID that was recorded after the SPE. The SEPS experiment has shown that the shape of the decay for the rigid fraction can be described by the Gaussian function. The HEPS was used for determining the T_2 relaxation for the soft fraction. The HEPS was also used for characterization of oil-extended EPDM, their vulcanizates and residual gel.

In addition to the HEPS, the T_2 relaxation decay was also measured for one of TPV samples using *the Carr−Purcell−Meiboom−Gill multiple-echo pulse sequence*: $90°_x - \{t_{CPMG} - 180°_y - t_{CPMG} -$ [acquisition of the amplitude of an echo maximum $A(t)$]$\}_N$, where t_{CPMG} was 4 ms and $N = 900$. This experiment has shown that the decay rate of oil molecules, which was measured by the HEPS, might be affected by the self-diffusion.

The longitudinal magnetization relaxation (T_1 relaxation time) was measured using *the inversion−recovery pulse sequence with the solid-echo detection* of the signal amplitude: $180°_x - t_{inv} - 90°_x - t_{se} - 90°_y - t_{se} -$ [acquisition of the amplitude of the echo maximum $A(t)$ as a function of t_{inv}].

To improve the selectivity of the T_2 relaxation experiments to different phases of TPVs, the usefulness of two different filters was evaluated. One filter was based on a use of a *180° inversion pulse followed by the HEPS*: $180°_x - t_{inv} - 90°_x - t_{He} - 180°_y - t_{He} -$ [acquisition of the amplitude of the echo maximum $A(t)$]. In this experiment, the longitudinal magnetization changes upon increasing the inversion time t_{inv} from a negative value through zero (the zero point) to the equilibrium magnetization. It will be shown below that the zero point for the rigid and soft fractions of the TPVs differs due to a low efficiency of the spin-diffusion, resulting in different T_1 relaxation behavior for rigid and soft fractions. The low efficiency of spin-diffusion is due to the large size of EPDM domains and the high molecular mobility in the EPDM/oil phase.

Other experiments explored a double quantum (DQ) dipolar filter. The proton DQ buildup curve for TPVs was recorded using the following pulse sequence: $[90°_x - t_{ex} - 90°_{-x}]_{EX} - [t_{DQ}]_{EV} - [90°_y - t_{ex} - 90°_{-y}]_{RE} - t_z -$ [$90°_x -$ (acquisition of the amplitude $A(t)$ of the transverse magnetization)]$_{DE}$. Subscripts EX, EV, RE, and DE stand for excitation, evolution, reconversion, and detection periods, respectively. The initial amplitude of the transverse magnetization $A(0)$, which was determined by a least-squares fit of the FID, was measured as a function of the excitation time, t_{ex}. The signal amplitude for soft materials is underestimated using this pulse sequence because resonance offsets and differences in the chemical shift for different types of protons are not compensated. Therefore, this pulse sequence was only used for estimating maximum position on DQ buildup curves.

A *DQ filtered Hahn−echo experiment* was performed using the pulse sequence below: $[90°_x - t_{ex}/2 - 180°_x - t_{ex}/2 - 90°_{-x}]_{EX} - [t_{DQ}]_{EV} - [90°_y - t_{ex}/2 - 180°_y - t_{ex}/2 - 90°_{-y}]_{RE} - t_z - [90°_x - t_{He} - 180°_y - t_{He} -$ [acquisition of the amplitude $A(t)$ of an echo maximum)]$_{DE}$. The first $90°_x$ and $90°_{-x}$ pulses in both pulse sequences excite DQ coherences that evolve for time t_{DQ}, which was set to 5 μs. The DQ coherences are converted by $90°_y$ and $90°_{-y}$ pulses to the z-polarization. The 180° refocusing pulses in the middle of the excitation and the reconversion periods eliminate the effects of resonance offsets and differences in the chemical shift for different types of protons.[31] After delay time t_z of the DQ filter, the HEPS was applied. It should be noted that the condition of selecting the isotropic powder average dipole−dipole interactions is broken for short DQ times. Simply, segments with (residual) coupling tensors oriented along B_o are selected first. Therefore, sufficiently long delay time t_z is required for proper redistribution of the magnetization between chains with different direction of the end-to-end vector with respect to the B_o. The redistribution of the magnetization is effective on distances that are comparable with the scale of spin diffusion and/or translational chain mobility within time t_z. The time t_z was set to 5 ms. The experiment with different t_z time has shown that 5 ms was sufficient for the redistribution of the magnetization over all rubbery chains either due to spin-diffusion or large spatial scale chain mobility.[32] Thus, by a proper choice of the excitation time, the decay of the transverse magnetization of phases with different molecular mobility and, consequently, in the strength of the dipole−dipole interactions can be selected.[33−38]

2.2.3. Analysis of the Phase Composition by the T_2 Relaxation Experiments. Analysis of the T_2 relaxation—the time dependence of the M_{xy} component of the macroscopic magnetization vector—is a valuable tool for the analysis of microphase composition and molecular motions in complex polymer materials.[26,39−41] The T_2 relaxation process is very sensitive to even small changes in molecular mobility, which can be seen from the range of T_2 for various materials: from about 8−20 μs for glassy and crystalline materials, to hundreds of microseconds—a few milliseconds for rubbery materials, tens of milliseconds for highly viscous liquids, and approximately a few seconds for low molar mass, low viscous liquids. The large difference in T_2 shows that this experiment is highly sensitive to a change in the chemical structure, composition, and morphology of polymer materials as reflected by a change in molecular motions. Because of the local origin of the NMR relaxation, the method can be applied to a selective study of different components/(inter)phases in polymeric materials if molecules/molecular fragments of those materials reveal a significant difference in molecular mobility. In this case, the T_2 relaxation function is a weighted sum of T_2 decays from different components/phases. The relative fraction of these components is proportional to the content of hydrogen in these (inter)phases/components. This allows obtaining accurate, quantitative data on the composition as well as characteristics of molecular motions in heterogeneous polymer materials.[26] It should be mentioned that the multicomponent relaxation does not always indicate microphase separation. For example, the rotational mobility of small molecules, which are homogeneously dispersed in a polymer matrix, could significantly differ from the mobility of polymer chains.

Analysis of the phase composition in complex polymeric materials using T_2 relaxation data is usually complicated due to several reasons: (1) *multiphase/component composition*; (2) *morphological heterogeneities* of materials, such as distribution of domain sizes resulting in a distribution of frequency of molecular motions; (3) *spatial heterogeneity of materials on the micrometer scale*, that is formed during processing, i.e., heterogeneous distribution of components, differences in morphology through the sample volume because of variation in temperature gradient and flow induced orientation in different parts of a sample, for example in skin layer vs core part; (4) *molecular-scale and morphological*

heterogeneity, which is caused by the chemical heterogeneity, such as molar mass distribution and a variation in the chain composition, chain sequences, and tacticity along a single chain; (5) *complexity of molecular motions* causing a complex shape of the decay of the transverse magnetization relaxation. Because of the reasons above, a thorough study of the T_2 relaxation as a function of temperature, both for a polymeric material and for the separate components that were used for its preparation, is desired for reliable data analysis.

2.2.4. The Shape of the Decay of the Transverse Magnetization Relaxation for Separate Components of TPVs. The decay of the transverse magnetization relaxation (T_2 decay) is caused by different mechanisms for rigid solids and highly mobile molecules. In rigid solids, the decrease of the transverse magnetization after an excitation does not require molecular motions and is caused by dipolar dephasing (coherent process). The T_2 relaxation of highly mobile molecules is due to stochastic modulations of local fields caused by molecular motions (incoherent process). Coherent and incoherent processes determine the T_2 relaxation for the intermediate motional regime.

Semicrystalline Polypropylene. At temperatures well above the dynamic glass transition (T_g^d) at the time scale of the NMR experiment, i.e., approximately 10−100 μs, the T_2 relaxation decay for semicrystalline polymers can usually be decomposed into three components, which originate from the crystalline phase, the semirigid crystal−amorphous interface and a soft fraction of the amorphous phase: short, intermediate and long T_2 relaxation times, respectively.[39−41] The theoretical description of the T_2 decay shape for semicrystalline polymers above T_g^d is still under debate and a purely phenomenological analysis of the decay shape with two or more components is commonly used. Different functions have been used for describing the T_2 decay for semicrystalline PP.[20,42−46] The shape of the relaxation component for the crystalline phase is described either by an Abragamian or a Gaussian function. A Gaussian, Weibull or an exponential function has been used to describe the T_2 relaxation of the crystal−amorphous interface. The relaxation of the soft amorphous fraction is described either with a single exponential or a sum of two exponential functions. It should be noted that the phase composition, as characterized by the NMR method, is affected to some extent by the temperature of the experiment[26] and by a fitting function used for the deconvolution of the T_2 decay into the separate components.[41,45,47,48] Nevertheless, the amount of rigid phase that is determined from the T_2 relaxation analysis corresponds rather well with crystallinity values obtained by other methods. It should be noted that, in general, different methods for crystallinity determination do not always yield the same results on exactly the same sample, because of the following reasons: (a) the complex morphology of semicrystalline polymers requires different sets of assumptions for the analysis of data recorded by the different techniques; (b) the two-phase model is rather simplified for describing semicrystalline polymers due to the presence of a crystal−amorphous interface, which can be detected either as crystalline or amorphous fraction depending on the method used; (c) the discrimination of the crystalline phase from the amorphous one is made on the basis of different characteristics, such as the enthalpy of melting (DSC), long-range periodicity (WAXD), bond vibrations (vibrational spectroscopy), the specific volume (density analysis), or molecular mobility (NMR).

EPDM. A quantitative analysis of the shape of the T_2 decay for elastomers is not always straightforward due to the complex origin of the relaxation function itself[49−54] and the structural heterogeneity of polymer networks.[13] A function that has been suggested for rubbers by J. P. Cohen-Addad,[55] and is hence referred as the Cohen-Addad function, describes rather well the shape of the T_2 decay for cross-linked rubbers. Adjustable parameter of this function (θ in eq 20 in ref 55) is related to the strength of the dipolar coupling, as determined by the second moment, M_2, of the NMR line shape. The Cohen-Addad function has the least number of fitting parameters as compared to other functions, which have been used. Therefore, this function was used in the present study although its theoretical validity is subject to discussion.[56] T_2 was determined from M_2 value using expression for a Lorentzian line shape, as provided in ref 60.

Oil. Below the critical molecular weight, the T_2 decay for oligomers and low-molecular-weight polymers is well described by an exponential function.[57] Above the critical molecular weight, the decay shape for polymer melts is similar to that of polymer networks because of the effect of chain entanglements on chain motions,[49,50,52] as well as the difference in molecular mobility of chain-end blocks and entangled part of a polymer chain.[58] Although the molecular weight of Sunpar 2280 oil is lower than the critical one, the shape of the T_2 decay deviates from the exponential one due to the molecular weight distribution.

2.2.5. Analysis of the NMR T_2 Relaxation Data for TPVs. EPDM/PP/Oil TPV. The shape of the T_2 decay for the separate components of the TPVs is already rather complex. Therefore, only a phenomenological analysis of the decay shape can be used in the present case. It will be shown below that EPDM, oil, amorphous, and crystalline phases of PP reveal a distinct difference in molecular mobility at temperatures above 100 °C, which allows selective characterization of the different fractions of the TPVs using the T_2 experiments. However, one should keep in mind that a single relaxation time for each fraction of the TPVs should be considered as the weight-average parameter of a distribution of apparent relaxation times. It is also important to mention that, due to the complex phase behavior of TPVs, the NMR relaxation components that are separated on the base of differences in molecular mobility do not necessary correspond to TPV fractions of different chemical structures.

The FID after the SPE was fitted with a linear combination of Gaussian and exponential functions, as it was discussed in part 2.2.2:

$$A(t) = A(0)^{cr} \exp[-(t(T_2^{cr})^2] + A(0)^{l} \exp[-t/T_2^{l}] \qquad (1)$$

Only the initial part of the decay in the time range from 0 to 100 μs was fitted. In this fit, the baseline was fixed to the value that was measured at the same conditions for the NMR tube without the sample. Superscripts in eq 1 stand for "cr" (*cr*ystalline phase) and "l" (*l*ong decaying part of the FID, which originates from the soft fraction of TPV composed of the amorphous PP, EPDM and oil). Since the T_2^l value, as determined from the SPE, is affected by B_o heterogeneity, this relaxation component cannot be used for the analysis of molecular mobility of the soft fraction of TPVs.

The decay of the transverse magnetization, as measured with the HEPS, was fitted with a linear combination of an exponential function, the Cohen-Addad function[55] and an exponential function:

$$A(t) = A(0)^{sa} \exp[-(t(T_2^{sa})] + A(0)^{r} f(CA)[-(t/T_2^{r})] + A(0)^{o} \exp[-t/T_2^{l}] \qquad (2)$$

Superscripts in eq 2 stand for "sa" (*s*oft *a*morphous PP phase), "r" (*r*ubbery EPDM phase) and "o" (*o*il fraction). The validity of the assignment of these relaxation components to different phases of the TPVs will be demonstrated below. The T_2 decay, as measured with the HEPS for oil-extended nonvulcanized EPDM, was fitted with a linear combination of two exponential functions:

$$A(t) = A(0)^{r} \exp[-(t(T_2^{r})] + A(0)^{o} \exp[-t/T_2^{o}] \qquad (3)$$

In the equations above, the time constants (T_2 relaxation time), which are characteristic of different slopes in the magnetization decay curve, are related to molecular mobility. The longer the T_2 relaxation time, the larger the frequency (and/or the amplitude) of the molecular motions. The relative fraction of the relaxation components, $\{A(0)^{index}/[A(0)^{cr} + A(0)^{sa} + A(0)^{r} + A(0)^{o}]\} \times 100\%$, as designated in the text by % T_2^{index}, represents the fraction of hydrogen in phases/components with different molecular mobility. Since the hydrogen content in PP, EPDM and oil is nearly the same, the % T_2^{index} represents the mass fraction of TPV fractions with different molecular mobility. Repeated experiments for the same

sample indicate that the relative error of the relaxation parameters was smaller than 5−10%.

2.2.6. Determination of the Molar Mass of Network Chains in Rubbers and Rubbery Phases. ^{1}H NMR T_2 relaxation in polymers at temperatures that are well above T_g^d is a measure for anisotropy of chain motions, or more precisely, residual dipolar couplings. The distinguishing feature of the T_2 relaxation for cross-linked polymers is the plateau observed at temperatures that are well above T_g^d.[13] The temperature-independence of T_2 in that plateau (T_2^{pl}) is attributed to constraints, which limit the number of possible conformations of a network chain relative to those of a free chain. Suggesting the Gaussian chain statistics, the theory of transverse relaxation in elastomeric networks relates T_2^{pl} to the number of statistical segments, Z, in the network chains that are formed by chemical and physical network junctions:[59,60]

$$Z = (T_2^{pl})/[a(T_2^{rl})] \quad (4)$$

where a is a theoretical coefficient which depends on the angle between the segment axis and the internuclear vector for the nearest nuclear spins at the main chains. For polymers containing aliphatic protons in the main chain, this coefficient is close to 6.2 ± 0.7.[60] T_2^{rl} is the relaxation time measured below T_g for the polymer swollen in a deuterated solvent. T_2^{rl} for swollen EPDM, as measured at −133 °C, is 10.4 ± 0.2 μs.[21] Using the number of backbone bonds in one statistical segment, designated as C_∞, the weight-average molar mass of network chains can be calculated from the Z value:

$$M_w = ZC_\infty M_u/n \quad (5)$$

Here M_u for EPDM is the average molar mass per elementary chain unit for the copolymer chains, and $n = 2$ is the number of backbone bonds in an elementary chain unit. A C_∞ value of 6.62 for an alternating ethylene−propylene copolymer[61] was used for the calculation of M_w of EPDM chains in TPVs.

For rubbers as such, the NMR method determines the total, volume average network density that is composed of chemical cross-links (CC), temporary (EN/TE) and trapped (EN/TR) chain entanglements.[21] For partially swollen samples at volume concentration of a solvent of approximately 40%, the NMR method determines the network density composed of CC and EN/TR.[21] The NMR analysis of a series of EPDM vulcanizates as such and those in the partially swollen state provides an estimate of the molar mass between apparent chain entanglements, M_e. The obtained M_e value of 1900 ± 200 g/mol is in the same range as those determined by other methods, which shows that the NMR method provides rather accurate values of the network density in EPDM rubbers.[21,62] Moreover, the T_2 relaxation analysis of several cross-linked rubbers has shown that M_w values, as determined from T_2^{pl}, coincide within 15−20% with M_w values that have been determined by traditional methods for network structure analysis, such as mechanical experiments, equilibrium swelling and the chemical conversion of functional groups involved in cross-link formation.[13,21,59,63] It should be mentioned that theories, which are used for calculating the network density from physical properties (such as equilibrium modulus, equilibrium swelling and T_2), are based on certain assumptions that are source of systematic errors. Possible artifacts in network structure analysis by the NMR T_2 relaxation method were recently discussed.[64−66]

3. Results and Discussion

The TPVs that are investigated in the present study are composed of *i*-PP, EPDM and paraffinic oil. The microphase structure of this material is rather complex due to semicrystallinity of PP and partitioning of the oil between the cross-linked EPDM and the amorphous phase of PP. Therefore, knowledge of the T_2 relaxation behavior of the separate TPV components is necessary for reliable analysis of the phase composition and molecular mobility in these materials. Proton NMR T_2 relaxation of PP was previously studied.[20,42−46] Molecular mobility and the network structure in oil-extended EPDM have been not previously analyzed in details. Therefore, we will start from this topic first.

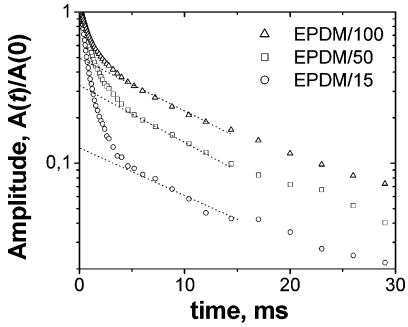

Figure 1. T_2 relaxation decay for oil-extended EPDM samples EPDM/12, EPDM/50 and EPDM/100 without added vulcanization additives. The T_2 decay was measured at 40 °C using the HEPS. The dotted lines, which are guide for the eye, mark the decay part that largely originates from the relaxation of oil molecules. The amplitude of the transverse magnetization, $A(t)$, was normalized to its value at time zero, $A(0)$.

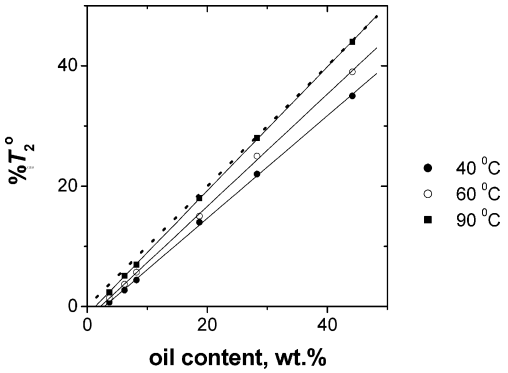

Figure 2. Dependence of % T_2^o on the oil content (in wt %) at different temperatures for oil-extended EPDM samples without added vulcanization additives. Solid lines are results of a linear regression analysis of the data. The dotted line of the slope one is a guide for the eye.

3.1. Molecular Mobility of Oil Molecules in Unvulcanized EPDM and EPDM Vulcanizates. It is well established that the physical state and molecular mobility of small molecules in a polymer can be strongly influenced by molecular mobility of the host matrix.[67−70] Highly selective characterization of EPDM chains and oil molecules in oil-extended EPDM can be performed only in the case when molecular mobility and consequently the T_2 relaxation of EPDM and oil is distinctly different. To determine the optimum temperature for the analysis, the T_2 relaxation experiment is performed at different temperatures for unvulcanized EPDM containing various amounts of oil. The T_2 decay for oil-extended EPDMs consists of fast and slow decaying components, as can be seen in Figure 1. The fast-decaying component is characterized by T_2 value of a few milliseconds. The other component has a substantially longer decay time. The characteristic decay time of these components (T_2^r and T_2^o) is comparable with that of pure rubber[21] and paraffinic oil. The relative fraction of the T_2^o component increases with increasing amount of oil in EPDM.

Below 90 °C, the relative fraction of the T_2^o relaxation component, % T_2^o, is lower than the amount of oil in the samples (Figure 2). This suggests that some oil molecules and/or their fragments are physically trapped in the EPDM matrix and/or oil coexists in different environments, i.e., oil-rich and EPDM-rich domains. At 90 °C, the % T_2^o coincides within the accuracy of the measurement with the amount of oil (in wt %) in oil-

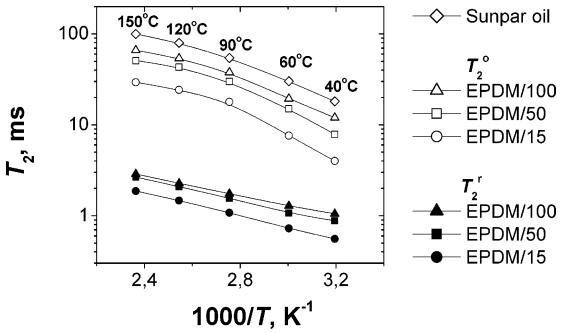

Figure 3. Temperature dependence of relaxation times T_2^r and T_2^o (close and open points, respectively) for oil-extended EPDM samples EPDM/15, EPDM/50, and EPDM/100 without added vulcanization additives, and paraffinic oil Sunpar 2280. The lines are guide for the eye.

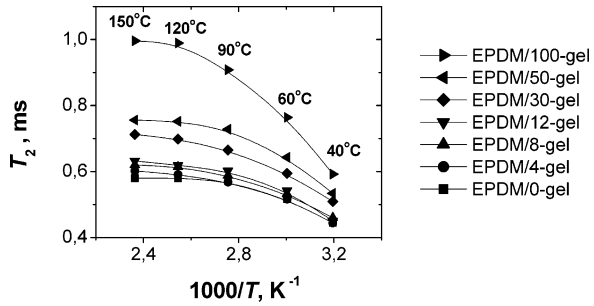

Figure 4. Temperature dependence of T_2^r for the gel fraction of oil-extended EPDM vulcanizates (see Table 1). Lines are guide for the eye.

extended EPDM. Thus, the molecular mobility of EPDM chains and oil molecules at 90 °C is decoupled to a large extent, and the relaxation times T_2^r and T_2^o can be used as a measure of molecular mobility of EPDM and oil. However, this assignment of the relaxation components is very simplified because of the following reasons: (1) the complex shape of the T_2 decay for EPDM and oil, which requires several assumptions for deconvolution of the T_2 decay into the relaxation components, as it was discussed in the Experimental Part; (2) molecular mobility of a small fraction of EPDM and oil could be rather similar due to a broad molar mass distribution (*MWD*) of EPDM and oil fractions; (3) EPDM chain-end fragments reveal molecular mobility and consequently a T_2 relaxation similar to that of oil; (4) the molecular mobility of EPDM chains and oil molecules is coupled to some extent even at high temperatures, as follows from the dependence of T_2^o on the sample composition (Figure 3).

The temperature dependence of theT_2 relaxation parameters for oil-extended EPDM is shown in Figures 2 and 3. Both T_2^r and T_2^o increase with increasing temperature due to an increase in the frequency and the amplitude of motions of EPDM chains and oil molecules. T_2^o is shorter for all oil-extended EPDMs than for pure oil. The difference increases with decreasing oil content (Figure 3). This means that EPDM chains hinder the molecular mobility of oil molecules due to a coupling of thermal motions of EPDM and oil. The amount of oil in EPDM affects also T_2^r. The T_2^r value increases with increasing amount of oil in EPDM, which is obviously due to a plasticization effect and a decrease in entanglement density, as will be shown below.

Upon vulcanization, T_2^r decreases because permanent cross-links increase the residual anisotropy of network chain motions. Vulcanization of EPDM samples causes an additional decrease in T_2^o, as will be shown below. The higher the network density, the shorter T_2^o. Thus, molecular mobility of oil molecules depends on (1) the anisotropy of EPDM chain motions and (2) the mesh size of network holes with respect to the radius of gyration of oil molecules. Translational mobility of oil molecules should be influenced by the availability of network holes (mesh size) that are sufficiently large compared to the size of oil molecules.

3.2. Effect of the Amount of Oil on the Entanglement Density in EPDM Vulcanizates. Chain entanglements provide a large contribution to the network density in EPDM vulcanizates.[13] Oil that is dissolved in EPDM increases the mean distance between neighboring EPDM chains causing a decrease in the entanglement density. To determine the effect of oil on the entanglement density, the network density was determined for EPDM vulcanizates that were cured in swollen state. The initial samples contained various amount of paraffinic oil, i.e., from 5 to 100 weight parts of oil per 100 parts by weight of EPDM (phr). The samples were cured at the same conditions with the same amount of vulcanization recipe per weight unit EPDM, which should result in nearly constant density of chemical cross-links for all series of the vulcanizates (Table 1). To simplify the analysis of the T_2 decay and improve the accuracy of the network density analysis, the oil was extracted from all vulcanizates.

The temperature dependence of the T_2 relaxation time for extracted vulcanizates (gels) as a whole is shown in Figure 4. Above 90 °C, T_2 reaches a nearly constant value contrary to nonvulcanized samples, which show a continuous increase in T_2 for EPDM chains (Figure 3). The temperature independence of T_2 for gels means that T_2 is hardly influenced by the frequency of chain motions and its value is determined by constraints that limit the number of possible conformations of network chains with respect to those of a free chain. The temperature independence of T_2 at the high-temperature plateau for the gels suggests also that the fraction of network defects, such as dangling chain-ends and chain loops, is low in the studied samples.[13]

The T_2 relaxation time at 90 °C is used for calculating the mean molar mass of network chains in gels, as described in the Experimental Part. Chemical cross-links, temporary and trapped chain entanglements contribute to the total network density, M_{c+en}, for gels as a whole.[13,21] The value of $1/2M_{c+en}$ for gels decreases with increasing amount of oil in the initial samples (Figure 5). The large decrease in the network density is due to a decrease in the entanglement density in gels, since the density of chemical cross-links should not largely influenced by the amount of oil in the initial samples. The decrease in the entanglement density can be due to a decrease in the density of temporary and/or trapped chain entanglements. To determine the effect of oil in the initial EPDM on the density of both types of chain entanglements in gels, the network density was also determined for partially swollen gels. Temporary chain entanglements vanish in partially swollen samples, which allows determining the density of both types of chain entanglements.[21]

The dependence of T_2 on the solvent content in the gels is shown in Figure 6. Swelling hardly influences T_2 for EPDM/0. This means that the fraction of temporary chain entanglements is low in this vulcanizate and that most of entanglements in the initial rubbers are trapped upon vulcanization. Contrary to EPDM/0, swelling largely affects T_2 of gels that that were cured in swollen state. Starting from a low solvent content, V_s, T_2 increases, which is mainly due to chain disentanglement.[21] [A slight decrease in the strength of the interchain proton dipole−dipole interactions could also cause a small increase in T_2 is swollen samples.] The increase is more pronounced for gels with larger oil fractions in the initial samples. Thus, the fraction

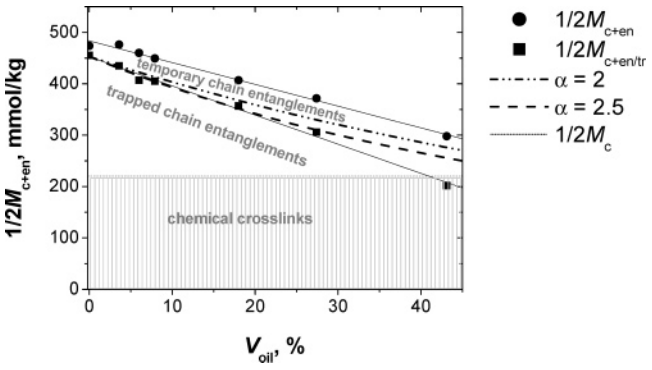

Figure 5. Density of chemical cross-links and chain entanglements ($1/2M_{c+en}$) in the gel fraction of oil-extended EPDM vulcanizates as a function of the volume fraction of oil in the initial samples, V_{oil}, for the gel fraction as a whole (●) and for partially swollen gels (■). $1/2M_{c+en}$ for partially swollen gels was calculated from T_2 at the maximum of the dependences in Figure 6. Solid lines represent the results of linear regression analysis for gels as a whole (intercept = 483 ± 4 mmol/kg; slope = −4.2 ± 0.2 mmol/(kg %); the correlation coefficient = 0.996); and for partially swollen samples (intercept = 453 ± 5 mmol/kg; slope = −5.7 ± 0.2 mmol/(kg %); the correlation coefficient = 0.997). Dotted lines are calculated using eq 6 for α values of 2 and 2.5.

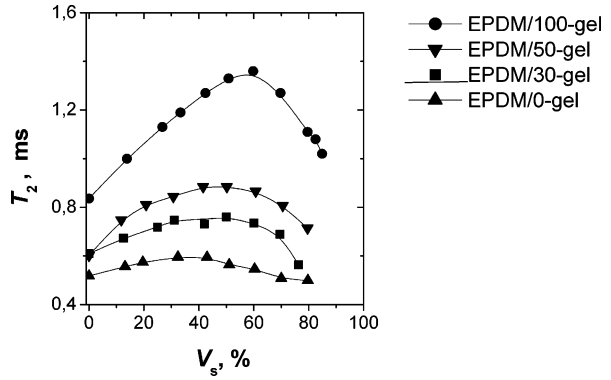

Figure 6. ^{1}H T_2^r relaxation time at 90 °C for the gel fraction of oil-extended EPDM vulcanizates as a function of the volume fraction of tetrachloroethylene in swollen gels, V_s. Lines are guide for the eye.

of temporary entanglements in gels as a whole largely increases with increasing oil content in the initial samples. At $V_s \approx 40-60\%$, T_2 reaches a maximum value. At higher values of V_s, T_2 decreases until a state of equilibrium swelling is reached. This decrease in T_2 is thought to reflect the increase in intrachain, proton dipole−dipole interactions as a result of network chain elongation upon a progressive increase in the solvent fraction in the swollen gel.[49]

The T_2 relaxation time at the maximum of dependence of T_2 on V_s (Figure 6) is mainly determined by the network density that is composed of chemical cross-links (c) and trapped chain entanglements (en/tr), $1/2M_{c+en/tr}$.[21] $1/2M_c$ for EPDM/0 vulcanizate was calculated using the following equation: $1/2M_{c+en} = 1/2M_c + 1/2M_{en}$, where $M_{en} = 1900 \pm 200$ g/mol.[21] The value of $1/2M_{c+en/tr}$ for swollen gels decreases with increase of oil content in the initial samples and approaches the density of chemical cross-links for EPDM vulcanizate with the largest amount of oil in the initial sample: EPDM/100 (Figure 5). Since the density of chemical cross-links, $1/2M_c$, for all samples should be close to its value for EPDM vulcanizate without oil (EPDM/0), chain entanglements are hardly present in swollen EPDM/100 gel. The density of temporary chain entanglements, $1/2M_{c+en/te}$, in gels as a whole can be determined by subtraction of the network density in partially swollen gels ($1/2M_{c+en/tr}$) from that in gels as a whole ($1/2M_{c+en}$). The density of temporary

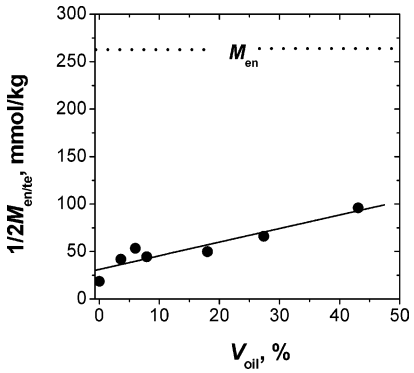

Figure 7. Density of temporary chain entanglements ($1/2M_{en/te}$) in the gel fraction of oil-extended EPDM vulcanizates as a function of the volume fraction of oil in the initial samples, V_{oil}. Solid line represents the result of a linear regression analysis: (intercept = 31 ± 5 mmol/kg; slope = 1.4 ± 0.3 mmol/(kg %); the correlation coefficient = 0.93). The dotted line shows the density of apparent chain entanglements in EPDM without oil.[21]

chain entanglements in gels as a whole slightly increases upon increasing oil content in the initial samples (Figure 7). However, $1/2M_{c+en/te}$ in gels is a few times lower than the entanglement density in EPDM without oil (Figure 7). This means that chemical cross-links in cured oil-extended EPDM largely hinder the formation of temporary chain entanglements upon extraction of oil from the vulcanizates.

The decrease in the entanglement density upon increasing oil content in the vulcanizates can be estimated using a scaling approaches.[71] In concentrated polymer solutions, the plateau modulus, G_o, and consequently the entanglement density is scaled with the volume fraction of polymer, ϕ, with an exponent α: $G_o \sim \phi^\alpha$. According to several experimental and theoretical studies the value of α varies from 1.9 to 2.5.[61,72−79] The effect of the amount of oil on the total network density in swollen gels was calculated using the following equation for α values of 2 and 2.5:

$$1/2M_{c+en} = 1/2M_c + 1/2M_{en}(1 - V_{oil})^\alpha \qquad (6)$$

The experimental dependence of $1/2M_{c+en}$ on V_{oil} for swollen gels could be described using scaling approach (Figure 5). Thus, the decrease in the overall network density in oil-extended EPDM vulcanizates upon increasing oil content is due to a decrease in the entanglement density.

3.3. Selective Characterization of PP, EPDM and Oil in TPVs Using Proton NMR T_2 Relaxation Analysis. The T_2 relaxation decay, which is measured with the SPE and the HEPS at elevated temperatures, reveals four fractions of the TPVs with distinct differences in molecular mobility, as reflected by T_2^{cr}, T_2^{sa}, T_2^r, and T_2^o values (see eqs 1 and 2). The differences are the most pronounced at 110 °C. Higher temperature for the experiments is not desired because the PP phase can be annealed during the measuring time.[20] As example, the T_2 decay for one of the samples is shown in Figure 8. At 110 °C, the T_2 values for these four TPV fractions are in the range that is typical for separate components of the TPVs, i.e., crystalline and amorphous phases of PP, EPDM vulcanizates and oil. The relative fractions of the relaxation components—% T_2^{cr}, % T_2^{sa}, % T_2^r, and % T_2^o (see eqs 1 and 2)—provides the amount (in percent of hydrogen atoms) of TPV fractions characterized by large differences in molecular mobility. In the entire range of the TPV compositions, the relative intensity of T_2^r and T_2^o relaxation components is close to the amount of EPDM and oil, respectively (Figure 9b,c). Crystallinity of PP, as determined by the

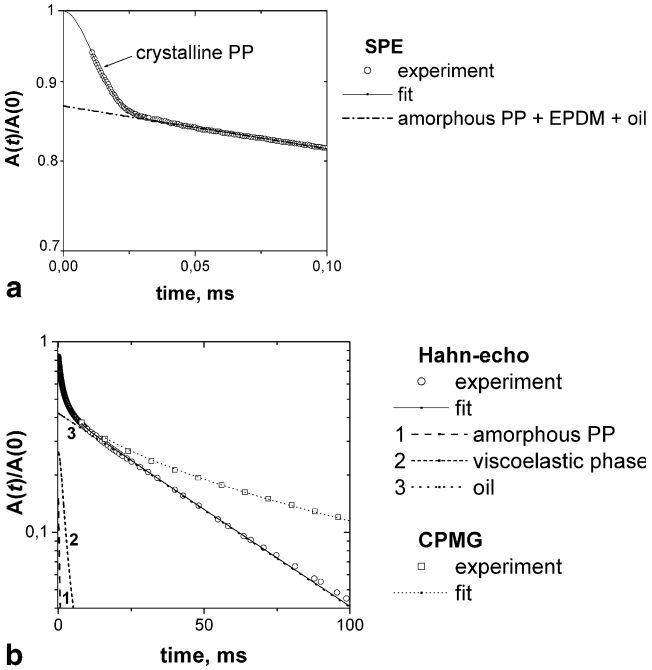

Figure 8. T_2 relaxation decay for TPV that is composed of 38.3 wt % EPDM, 38.3 wt % oil, 16.4 wt % PP and 7.0 wt % peroxide based vulcanization recipe. The decay was measured at 110 °C. Key: (a) FID that was measured with the SPE; (b) the T_2 relaxation decay for the soft fractions of the TPV, as measured with the HEPS and CPMG. The amplitude of the transverse magnetization, $A(t)$ from all experiments, was normalized to the initial amplitude of the transverse magnetization, $A(0)$, that was determined by a least-squares fit of the FID measured by the SPE. The solid line represents the result of a least squares adjustment of the decays using eqs 1 and 2 for the SPE and the HEPS data. The CPMG data were fitted with the Weibull function. Dotted lines show separate components.

NMR method at 110 °C,[20] is hardly affected by the TPV composition and is close to 70 wt %. The value of (% T_2^{cr} + % T_2^{sa}) is also close to the amount of *i*-PP in the TPV with exception of samples with the lowest and the highest content of *i*-PP (Figure 9a). The deviations from the sample composition could find the following explanation. The NMR relaxation components that are separated on the base of differences in molecular mobility do not necessary correspond to TPV fractions of different chemical structures, because of the complex phase behavior of TPVs, namely: (1) partitioning of oil between PP and EPDM phases, (2) small fraction of rubbery-like atactic PP, and (3) partial miscibility of propylene-rich chain fragments of EPDM with amorphous PP phase at EPDM/PP interface.

The results in Figure 9 suggest a good phase separation of the PP and EPDM phases and decoupling of molecular mobility of oil molecules from chain mobility of the host matrix for most of the samples. Therefore, the following assignment of the T_2 relaxation components to different morphological structures in TPV can be made: (1) T_2^{cr} relaxation, crystalline PP and a rigid fraction of the crystal−amorphous PP interface; (2) T_2^{sa} relaxation, mainly the soft fraction of amorphous PP, small amounts of propylene-rich chain fragments of EPDM at the PP/EPDM interface and a small fraction of oil molecules that are immobilized in the amorphous phase of PP; (3) T_2^{r} relaxation, mainly EPDM rubber, possibly small amounts of the atactic fraction of PP at the PP/EPDM interface, and the least mobile oil molecules; (4) T_2^{o} relaxation, highly mobile oil molecules. It should be mentioned that the distinct T_2 relaxation for oil molecules does not suggest microphase separation. It is shown above that the rotational mobility of oil molecules is largely decoupled from mobility of EPDM chains at temperatures above

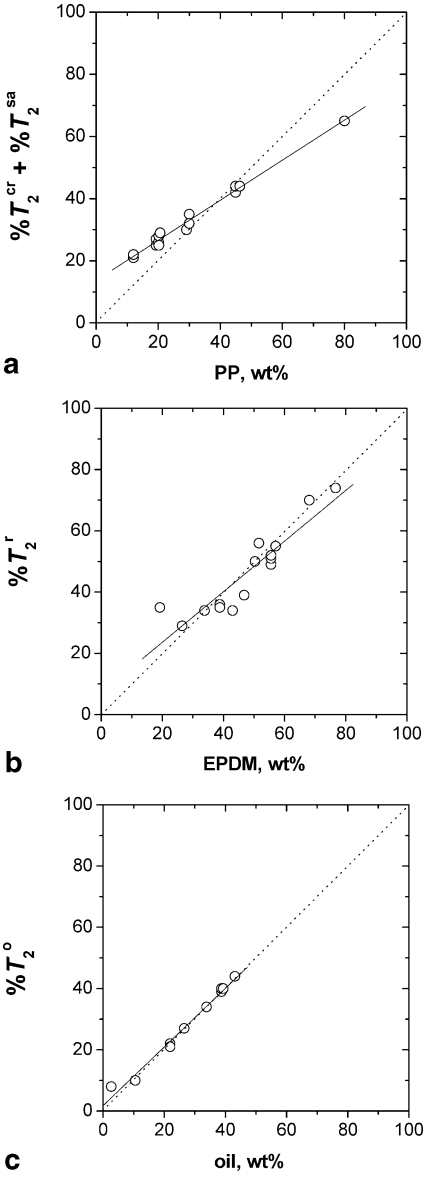

Figure 9. Dependence of the relative intensity of the T_2 relaxation components on weight fraction of PP (a), EPDM (b), and oil (c) in the TPVs. Key: (a) the sum of the relative fractions of T_2^{cr} and T_2^{sa} relaxation components against the weight fraction of *i*-PP in the TPVs; (b) the relative fraction of T_2^{r} relaxation component against the weight fraction of EPDM in the TPVs; (c) the relative fraction of T_2^{o} relaxation component against the weight fraction of oil in the TPVs. Dotted lines of the slope 1 are guide for the eye. Solid lines represent the result of a linear regression analysis of the data: (a) intercept = 13.7 ± 0.8%, slope = 0.64 ± 0.02, the standard deviation = 1.4%, the correlation coefficient = 0.993; (b) intercept = 7 ± 5%, slope = 0.83 ± 0.1, the standard deviation = 5.6%, the correlation coefficient = 0.917; (c) intercept = 1.8 ± 1.3%, slope = 0.96 ± 0.04, the standard deviation = 1.7%, the correlation coefficient = 0.992.

90 °C. Thus, the T_2 relaxation analysis at 110 °C provides selective information on molecular mobility of EPDM chains in the rubbery phase, of oil molecules, and of the amorphous and crystalline phases of PP.

3.4. The Effect of TPV Composition on EPDM Network Density. The relaxation time T_2^{r}, which mainly characterizes the EPDM chains in the rubbery phase of TPVs, can be used for quantitative determination of the network density in this phase. Several types of network junctions can contribute to the total network density, as determined by the NMR method. According to our previous studies, the NMR method measures the total network density that is composed of chemical cross-

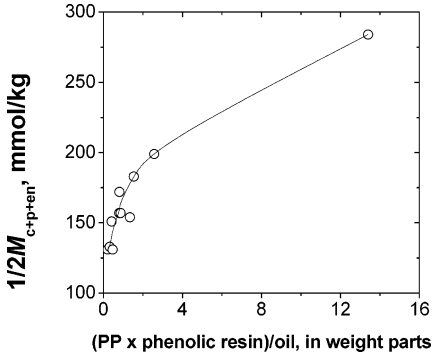

Figure 10. Network density in the rubbery phase of TPVs as a function of weight ratio PPx(phenolic resin)/oil. Solid line is a guide for the eye.

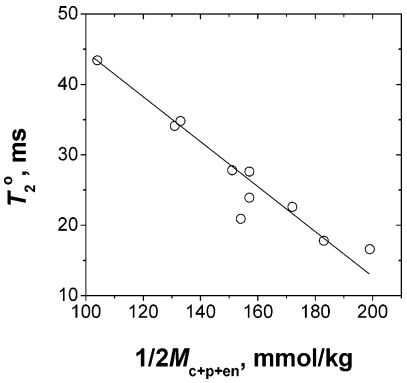

Figure 11. T_2 relaxation time for oil molecules at 110 °C as a function of the network density in the rubbery phase of TPVs. The solid line is a guide for the eye.

links and various types of physical network junctions.[13,21,80−83] In TPVs without oil (samples 7−11), the network density in the rubbery phase, $1/2M_{c+p+en}$, should be composed of chemical cross-links (c), physical junctions at the EPDM/PP interface (p), temporary (en/te), and trapped (en/tr) chain entanglements (en).

One could expect the following effect of TPV composition on the network density in the rubbery phase. The density of chemical cross-links should increase with the amount of phenolic resin until complete conversion of the third monomer of EPDM is reached. The entanglement density should decrease upon increasing the amount of oil. The density of temporary chain entanglements in TPVs containing a large fraction of oil should be low, as was shown above for oil-extended EPDM vulcanizates. One might expect that the density of physical junctions that originate from the EPDM/PP interface will increase with increasing relative amount of PP in the TPVs. The interfacial layer is formed at the shell of the rubber particles and PP particles occluded in the EPDM phase. Occlusion of PP particles in the dispersed EPDM phase has been suggested previously.[7] It should also be noted that the particle size of the rubbery phase is affected by the composition of TPVs.[6]

The network density for the full series of TPVs is shown in Table 3. Similar to oil-extended EPDM samples, the total network density in the TPVs increases with decreasing amount of oil in samples with comparable amount of PP and cross-linker (TPV5 vs TPV12, and TPV7 vs TPV13). For samples with the same amount of oil and PP (TPVs 1−3), the total network density increases by ≈20% upon a four times increase in the amount of cross-linker per unit weight of EPDM. For samples without oil and with the same amount of cross-linker per unit weight of EPDM (TPVs 7−10), the network density increases by 1.5 times with increasing amount of PP from 20.1 wt % to 80 wt %, which could be due to the following reasons. (1) Although EPDM and PP are demixed, propylene-rich chain fragments of EPDM would have a tendency to be partially mixed with the PP phase, resulting in a thin PP/EPDM interfacial layer of (sub)nanothickness. EPDM chain units that are trapped at the interface form physical network junctions. (2) EPDM chain fragments might also be trapped at the interfacial layer because of entanglement of PP chains with propylene-rich chain fragments of EPDM. (3) A change in the dimensions of the EPDM phase, the size and the number of PP occlusions in the EPDM phase should also cause a change in the interfacial EPDM/PP surface area per unit volume of EPDM and, consequently, in the density of physical EPDM/PP junctions.

Analysis of the total network density ($1/2M_{c+p+en}$) for the entire set of samples does not reveal a good correlation between the network density and the relative amount of either the cross-linker, the oil or the PP. This suggests that all types of network junctions, as indicated above, contribute to $1/2M_{c+p+en}$ in the rubbery phase of TPVs. Therefore, the total network density in the rubbery phase of TPVs is plotted in Figure 10 against the following weight ratio: [PP × (phenolic resin)]/oil. The use of this ratio has the following reasons. The increase in the amount of cross-linker and PP causes an increase in the density of chemical cross-links and physical network junctions at the EPDM/PP interface, respectively. The decrease in the amount of oil causes an increase in the entanglement density. Therefore, this weight ratio could be considered as a parameter that *qualitatively* relates the sample composition to the total network density in the rubbery phase of TPVs. The dependence in Figure 10 reveals a good correlation between the network density in the rubbery phase of TPVs and the "cross-linking" parameter. Thus, both chain entanglements, chemical and physical network junctions should be taken into account for analysis of viscoelastic properties of TPVs as a function of TPV composition.

3.5. The Effect of TPV Composition on the Phase Composition and Molecular Mobility in Different Phases of TPVs. It was shown above that the amounts of TPV fractions [(% T_2^{cr} + % T_2^{sa}), % T_2^{r}, and % T_2^{o}], which reveal different chain mobilities, are close to the sample composition (Figure 9). This suggests a good separation of PP and EPDM phases. Therefore, the T_2 relaxation time for different phases/components of TPVs provides phase selective information about molecular mobility in the TPVs. This information could be important for better understanding of the macroscopic properties of these materials and establishing structure-properties relationships. Some discussion of these items is given below.

The relaxation time for oil molecules, T_2^{o}, decreases with increasing network density in the rubbery phase (Figure 11). The shorter T_2, the smaller is the amplitude and/or frequency of molecular motions. It is anticipated that molecular mobility of small molecules in the polymer matrix is coupled to chain mobility.[84−86] Since translational and rotational mobility of oil

Table 3. Total Density[a] of Cross-links in the EPDM Phase of TPVs, as Determined from T_2^r

TPV	1	2	3	4	5	6	7	8	9	10	11	12	13	14	15
$1/2M_{c+p+en}$	151	172	183	133	199	284	237	265	287	359	157	131	104	157	154

[a] The total network density, $1/2M_{c+p+en}$ (in mmol/kg) is composed of chemical cross-links (c), chain entanglements (en) and physical network junctions (p) originating from EPDM/PP interface.

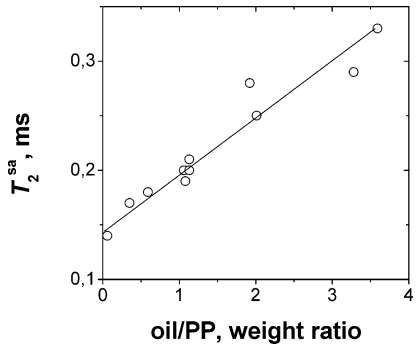

Figure 12. T_2 relaxation time of the soft fraction of PP at 40 °C as a function of mass ratio oil/PP. The solid line is a guide for the eye.

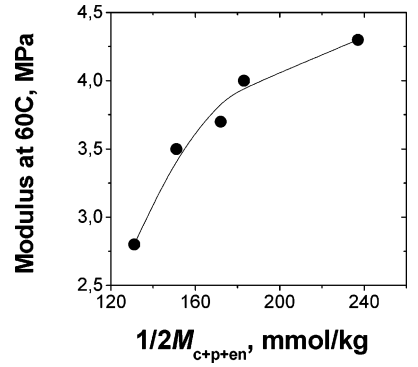

Figure 13. Modulus at 60 °C for TPVs containing 20 wt % PP against the network density of EPDM. The solid line is a guide for the eye.

molecules, as determined by the T_2^o value, correlate well with the network density (Figure 11), the dependence of T_2^o on $1/2M_{c+p+en}$ suggests that the majority of oil molecules resides in the EPDM phase at 110 °C. A small fraction of oil molecules is mixed with PP, since molecular mobility in the amorphous phase of PP increases with increasing oil/PP weight ratio, as can be seen in Figure 12. Plasticization of the amorphous PP by oil has also been shown previously by DMTA,[8] DIES,[12] and DSC.[14]

3.6. Some Relationships Between TPV Composition and Mechanical Properties. Mechanical properties of the TPVs are affected by a number of factors: (1) the sample composition; (2) morphological characteristics, such as domain sizes; (3) molecular characteristics of different phases, such as network density in a rubbery phase, crystallinity of PP and softness of the amorphous PP phase. Establishing structure-properties relationships for TPVs requires a multidisciplinary approach, which is outside the scope of the present study. Nevertheless, a few trends can be mentioned. The modulus of TPVs with the same PP content (samples 1−3, 7,13) increases from 2.8 to 4.3 MPa upon nearly two times increase in the network density in the EPDM phase (Figure 13). The modulus is largely determined by the fraction of PP in the samples, as can be seen in Figure 14. Its value increases from about 1 to 30 MPa with increasing PP content from 12 to 45 wt %. Thus, the network density in the rubbery phase of TPVs moderately influences the modulus. Both compression and tensile sets, which are determined 4 h after stress was removed, increase with the increase of PP content. These properties are only slightly affected by the network density in the rubbery phase. The increase in the network density in the rubbery phase improves elastic recovery both after compression and tensile deformations. Elastic recovery at short recovery time is somewhat faster for samples with larger oil fractions.

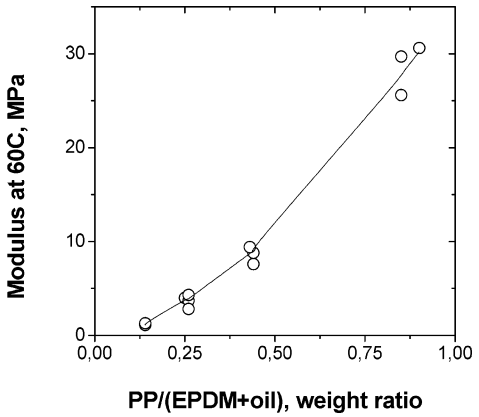

Figure 14. Modulus of TPVs at 60 °C as a function of the weight ratio PP/(EPDM + oil). The solid line is a guide for the eye.

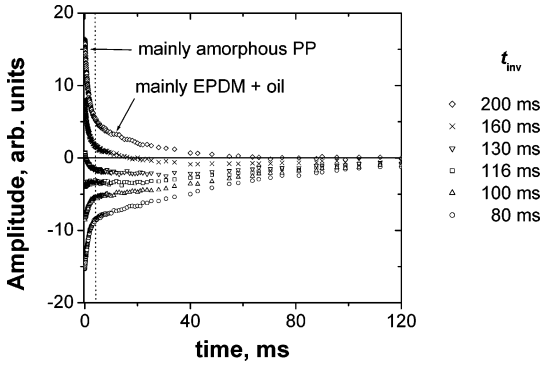

Figure 15. T_2 relaxation decays for TPV composed of 31.4 wt % EPDM, 31.4 wt % oil, 31.4 wt % PP and 5.8 wt % peroxide based vulcanization recipe. The decays are measured with the HEPS at different time, t_{inv}, after the 180°-inversion pulse. The experiment is performed at 110 °C. The inversion time is shown on Figure. The time domains, which mainly correspond to the relaxation of soft amorphous PP and the rubbery phase with oil, are shown by dotted line.

3.7. Possibilities for Improving the Selectivity of Proton NMR to Different Phases in TPV. Although the T_2 relaxation method, that is described above, offers rather good selectivity to different phases/components of the TPVs, the method involves elaborated least-squares analysis of the data that could hamper a wide method application. To enhance the selectivity of the T_2 relaxation to the analysis of different phases in TPVs, as well as to improve the accuracy of the data, two types of NMR filters are evaluated in the present study. The experiments are based on an inversion−recovery and a double quantum (DQ) filter followed by the HEPS.

If the size of domains exceeds a few hundreds of nanometers, the recovery of the longitudinal magnetization (T_1 relaxation, as measured by the inversion−recovery experiment) for rigid and soft fractions of two-phase polymers usually differs in a wide temperature range.[40] The efficiency of the ^{1}H spin-diffusion between PP and EPDM/oil phases in the TPVs is low due to the large size of EPDM domains, which is in the micrometer range, and high molecular mobility in the EPDM/oil phase. Therefore, differences in ^{1}H T_1 relaxation of PP and EPDM/oil phases could be explored to enhance the selectivity of proton NMR for the analysis of these phases in the TPVs. The T_2 relaxation decay that is measured with the HEPS after different inversion time (t_{iinv}) in the inversion−recovery experiment is shown in Figure 15. It is noted that the T_2 decay for crystalline PP is not detected by the HEPS. At short t_{inv}, the amplitude of the T_2 decay is negative. The initial amplitude of the decay $A(0)$ changes from a negative value through zero (zero point) at $t_{inv} \approx 95$ ms to the equilibrium magnetization upon increasing the

inversion time t_{inv}. Large changes in the shape of the relaxation decay are observed at values of t_{inv} that are close to the zero point. At $t_{inv} \approx 116$ ms, the T_2 relaxation component that originates from amorphous PP goes through the zero point and the transverse magnetization mainly originates from the relaxation of EPDM and oil. At $t_{inv} \approx 160$ ms, the zero point is observed for EPDM and oil. A global fit of the T_2 relaxation function at all range of t_{inv} can largely increase the accuracy of determination of the T_2 relaxation time for the TPV phases. The global fit, as described previously,[81,83] adjusts one T_2 value for each relaxation component that is common for all T_2 decays in the array. The important improvement of the global fit, as compared with a separate fit of each decay, is the high reliability of the "best fit" values of T_2. Although the inversion method can provide accurate values of T_2 for each phase of TPVs, the method requires elaborated data analysis and suffers from a lack of selectivity for EPDM and oil.

The other way of enhancing the selectivity explores a DQ filter. In the past decade, DQ and multi quantum (MQ) proton NMR experiments have been applied for characterization of polymer networks,[32,87−93] heterogeneity of grafted layers[94] and mobility of soft blocks in block copolymers.[95] Recently, DQ filters have been applied in spin-diffusion experiments for selection of the magnetization of a rigid phase in heterogeneous polymers.[33−38] In the present study, the DQ filter will be used to enhance the selectivity of the T_2 relaxation experiment to different phases in TPVs, as well as to gain qualitative information about the molecular scale heterogeneity of the rubbery phase in TPVs.

Using the DQ filter, the PP and EPDM phases in TPV can be selected by a proper choice of the excitation/reconversion time, t_{ex}. To determine the optimum t_{ex} for selecting different phases of TPVs, a DQ buildup curve is recorded. The initial amplitude of FID in the DQ experiment is shown as a function of the excitation time t_{ex} at short, intermediate and long values of t_{ex} (Figure 16 a−c). It is noted that the amplitude of the NMR signal in the DQ experiments should be smaller by at least 50% than its value in the SPE experiment. The DQ buildup curve shows two pronounced maxima. The first maximum is observed at $t_{ex} \approx 13.5$ μs. Such short excitation time is typical for crystalline phases in semicrystalline polymers.[38] Therefore, this maximum is assigned to crystalline PP. Our previous study of HDPE has revealed that the amorphous phase of HDPE shows an ill-defined maximum at $t_{ex} \approx 25$ μs.[38] Similar to HDPE, the amorphous phase of PP does not show a distinct maximum. The second broad maximum is observed at approximately 0.6 ms (Figure 16b). This maximum originates from EPDM network chains. Upon increasing t_{ex}, the transverse relaxation causes a decrease in the amplitude of the DQ filtered signal.[87] At long excitation times only the signal from more mobile chain fragments is measured.[34] Therefore, the gradual decay of the initial amplitude of the DQ signal at long t_{ex} might be assigned to network defects, such as loosely cross-linked EPDM chains, dangling chains and chain loops (Figure 16c). Long-chain network defects should have anisotropic chain mobility as opposed to, e.g., the oil. The absence of a pronounced maximum is an indication of a broad distribution of residual dipole−dipole couplings due to various types of network defects. The signal at long excitation times could also be caused by single quantum coherences that pass through the DQ filter due to imperfections of the radio frequency pulses and chemical shift effects. Therefore, identification of the origin of the signal at excitation times longer than a few milliseconds requires an additional study.

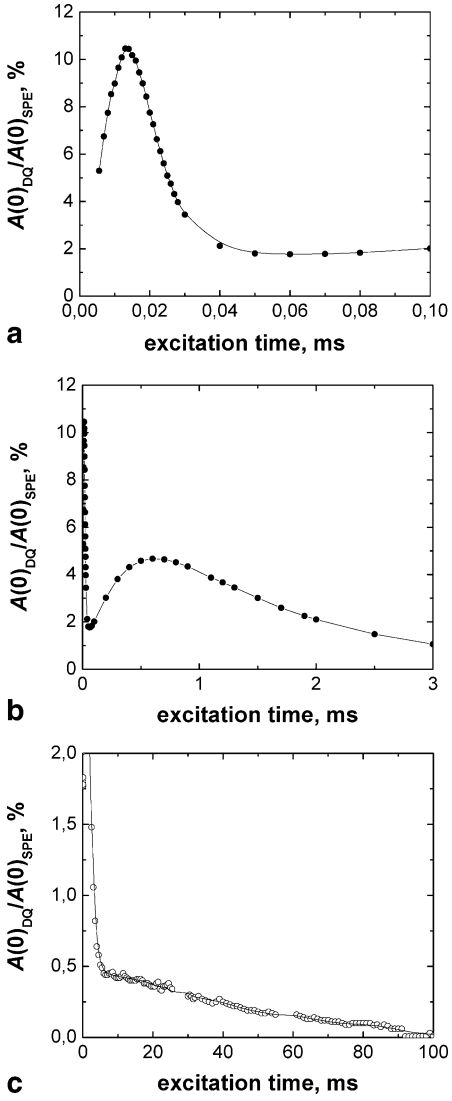

Figure 16. Proton DQ buildup curve at 110 °C for TPV that is composed of 38.3 wt % EPDM, 38.3 wt % oil, 16.4 wt % PP and 7.0 wt % peroxide based vulcanization recipe. The initial amplitude of FID in the DQ experiment, which is measured after t_z delay time, is shown as a function of the excitation time t_{ex} at short (a), intermediate (b), and long (c) values of t_{ex}. The amplitude is normalized to the initial amplitude of the transverse magnetization, $A(0)$, that was determined by a least-squares fit of the FID measured by the SPE without the DQ filter. The maxima at 13.5 μs and 600 μs correspond to crystalline PP and EPDM, respectively (Figure 16a and 16b). Gradual decay of the initial amplitude in Figure 16c might originate from EPDM network defects. To estimate the position of maximum both for rigid and soft fractions of the sample, the DQ buildup curves are recorded using the DQ experiment without 180° pulses (see part 2.2.2) that compensate the effect of resonance offsets and differences in the chemical shift for different types of protons of the rubbery phase. Therefore, the signal amplitude for this phase (Figure 16a,b) is underestimated in this experiment.

The mean decay time in the DQ filtered HEPS depends largely on t_{ex}. The normalized decay at different t_{ex} is shown in Figure 17a. This figure illustrates that the decay shape is not strongly influenced by t_{ex}, whereas the decay time increases with increasing t_{ex}. It should be mentioned that the observed decay shape is typical for polymer networks.[49−54] The efficiency of the DQ filter depends to a large extent on t_{ex}, as can be seen in Figure 17b,c. In these plots, the DQ filtered T_2 decays are normalized to the initial amplitude of the T_2^r relaxation component, $A(0)^r$ (see eq 2), that is measured by the HEPS without the filter. The initial amplitude of the normalized decays, $A(0)/A(0)^r$, is significantly lower than $A(0)^r$ determined by the

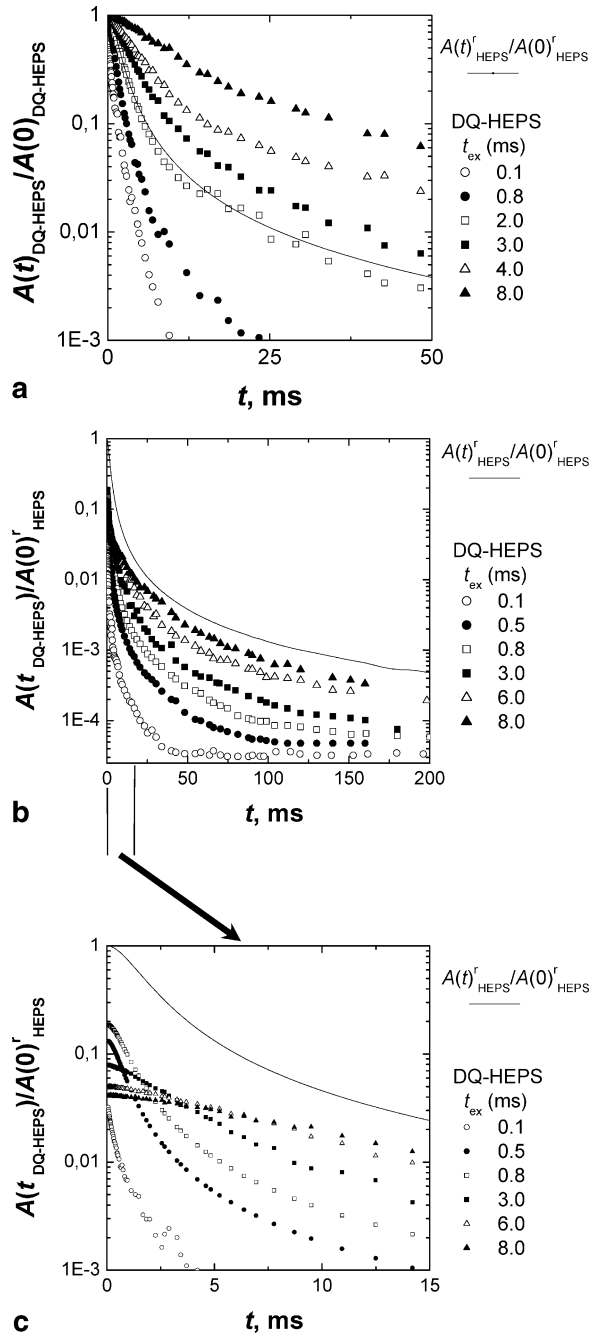

Figure 17. Decays of the transverse magnetization for TPV that is composed of 38.3 wt % EPDM, 38.3 wt % oil, 16.4 wt % PP and 7.0 wt % peroxide based vulcanization recipe. The T_2 decays (points) are measured at 110 °C with the HEPS after the DQ filter with different t_{ex}. The T_2^r relaxation component is shown by solid line. The T_2^r relaxation component (see eq 2) is determined by the analysis of the HEPS data measured without the DQ filter. Key: (a) The T_2 decays are normalized to the initial amplitude $A(0)$ of each decay. The $A(0)$ is determined by the least-squares fit of each decay with the Cohen-Addad function.[55] (b) The amplitude of the DQ filtered T_2 decays is normalized to the initial amplitude $A(0)^r$ of the T_2^r relaxation component. (c) The part of the decays from Figure 17b is shown at short decay times.

HEPS without the DQ filter. It is interesting to note that the maximum for the DQ build up curve for the EPDM phase is observed at 0.6 ms (Figure 16b). However, the mean decay time in the DQ filtered experiment at $t_{ex} = 0.8$ ms, is significantly shorter than that for the EPDM phase in the HEPS experiment without the filter (Figure 17a). Only at $t_{ex} = 2$ ms, the decay time from both experiments coincides. The dependence of the mean decay time on t_{ex} could be explained by heterogeneity of EPDM network structure. If the molar mass distribution of network chains would be narrow, the T_2 decays in the DQ filtered HEPS should not show large dependence on t_{ex}. Since network heterogeneity strongly influences the rate of buildup of the DQ coherences,[32,91] the dependence of the decay time on t_{ex} could be explained by a wide molar mass distribution of network chains in the EPDM phase of the TPVs.

Four different types of rubbery networks should be treated separately in discussion of network structure, network heterogeneity, chain entanglements and residual dipole−dipole interactions as measured by NMR methods: (1) cross-linked rubbers as such, (2) rubbers that are swollen after cross-linking, (3) rubbers that are cross-linked in swollen state as in the present study, and (4) the third type of rubbers after solvent is removed. In addition to that the type of curing method (e.g., conventional vulcanization and end-linking reactions) and the type of network junctions (e.g., their bulkiness and ziplike network junctions[13,63]) can largely influence the network topology, network heterogeneity, and the amount of network defects. These structural characteristics of polymer network could largely influence volume average chain dynamics and macroscopic properties. Results that are provided below are obtained for sample, which is cross-linked in swollen state and contained large amount of oil before cross-linking (EPDM:oil weight ratio equals 1). At this concentration of oil, EPDM chains are hardly entangled, as can be seen in Figure 5. Therefore, mobility of short and long chains, as well as network defects, is largely decoupled. Moreover, the experiments are performed at 110 °C. At this temperature, T_2 value for cross-linked EPDM is mainly determined by the length of network chains, as it follows from comparison the network density that was measured for the same series of samples by four different methods, i.e., analysis of stress−strain curves, equilibrium swelling, FT-Raman spectroscopy, and the T_2 relaxation analysis.[21] It is noted that the interpretation of the DQ filtered HEPS experiment that is provided below is not necessary applicable to other types of rubber networks (types 1, 2, and 4).

The relationship between the molar mass distribution of EPDM network chains and T_2 values, which are measured by the HEPS without and with the DQ filter, is schematically shown for TPVs in Figure 18. The shorter network chains, the larger the anisotropy of chain motions and the shorter T_2.[13] The opposite change should be observed for oligomers and linear polymeric chains; i.e., T_2 decreases with increasing molar mass due to a decrease in the frequency of molecular motions and the effect of chain entanglements.[57,58] Since the efficiency the DQ filter largely depends on the strength of the dipole−dipole interactions (see, e.g., Figure 16), the contribution of short and long EPDM network chains to the T_2 decay should depend on the excitation time. At short t_{ex}, the DQ filter enhances the contribution to the T_2 decay from short network chains those mobility is more anisotropic than that of longer network chains. The contribution of long network chains to the T_2 decay increases with increasing t_{ex}. Thus, at each particular t_{ex}, the DQ filter selects network chains with a certain range of molar masses. Since the T_2 relaxation time for EPDM at temperatures well above T_g is proportional to the molar mass of network chains (see eqs 4 and 5),[21] the range of T_2 values as a function of t_{ex} in the DQ filtered experiment may be used as a relative measure of the width of the molar mass distribution of network chains. It may be suggested that T_2, which is measured at the maximum of the build up curve for the EPDM phase (Figure 16b, $t_{ex} = 0.6$ ms), corresponds to the number-average molar mass of network chains. Contrary to the DQ filtered HEPS, all

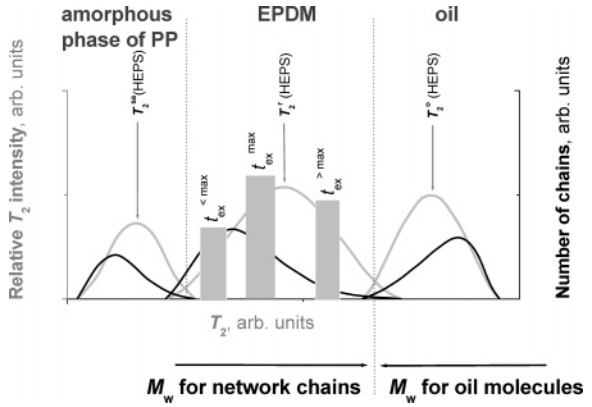

Figure 18. Schematic drawing that shows the molecular origin of T_2 relaxation time components for the soft fractions of TPVs. Distribution of T_2 relaxation time and molar mass distribution are shown by gray and black colors, respectively. The drawing explains differences in the initial amplitude and the decay time that are measured using the HEPS and the DQ filtered HEPS experiments for EPDM chains. Arrows with T_2^{index}(HEPS) indicate T_2 values that are measured using the HEPS for amorphous PP phase, EPDM and oil (see eq 2). It is noted that T_2, which is measured by the HEPS, is the weight-average characteristic of molecular mobility for each fraction of TPVs, since the relative contribution of a molecule and a network chain (either between chemical cross-links or physical network junctions) to the T_2 relaxation for each TPV fraction is proportional to the number of protons attached to this molecule and the network chain. The shaded area shows a part of the T_2 distribution for EPDM chains that is selected by the DQ filter at different excitation time, t_{ex}. The excitation time that corresponds to the maximum of the buildup curve for EPDM network chains (see Figure 16b) is indicated by t_{ex}^{max}.

EPDM chains contribute to the T_2 that is measured by the HEPS without the DQ filter. Since the relative contribution of a network chain to the total relaxation function of heterogeneous network is proportional to the number of protons attached to this chain, the weight-average molar mass of network chains is measured by the HEPS without the filter.

Another parameter that characterizes the molar mass distribution is the initial amplitude $A(0)$ of the DQ filtered Hahn-echo decay. $A(0)$ undergoes the following changes upon an increase of t_{ex} (Figure 17b,c and 19). Starting from a low value of t_{ex}, $A(0)$ increases, reaches a maximum and decreases at longer values of t_{ex}. It could be suggested that the dependence of $A(0)$ and T_2 on t_{ex} (Figure 19) can be used to reveal relative differences in the shape of a function describing the molar mass distribution of network chains for a series of samples prepared with the same vulcanization recipe. However, the quantitative analysis on the molar mass distribution is complicated, because $A(0)$ is influenced by two opposite effects: (1) a decrease in the anisotropy of chain motions upon increasing the length of network chains, which reduces the contribution of longer chains to the DQ transitions; (2) an increase in contribution of longer network chains to $A(0)$ due to larger number of protons born by longer chains. Moreover, one cannot exclude two other effects that could influence the dependence of $A(0)$ on t_{ex} as well: (1) the effect of a wide spectrum of the frequencies of molecular motions of polymer chains in general, and (2) a gradient in molecular mobility along a network chain, i.e., a loss of restrictions of rotational and translational mobility of a chain unit when moving away from the network junction. Therefore, the analysis of the dependence of $A(0)$ and T_2 on t_{ex} in the relation to network heterogeneity requires additional intricate studies. The origin of the network heterogeneity—either on the molecular or (and) larger scale—should be the topic of a separate study. The effect of chain entanglements on results of the DQ filtered T_2 relaxation experiments should also be studied, since the presented data are obtained for EPDM, which is cross-linked in swollen state resulting in very low entanglement density.

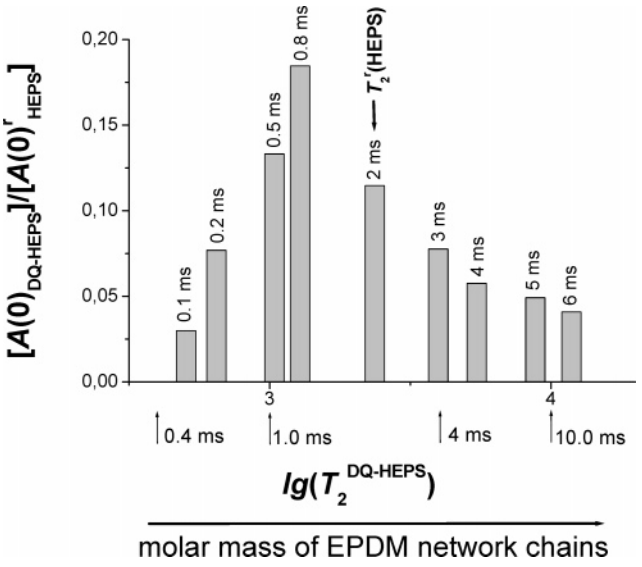

Figure 19. T_2 relaxation time distribution in the DQ filtered HEPS experiment that is performed at 110 °C for EPDM network chains in EPDM/PP TPV. The TPV is composed of 38.3 wt % EPDM, 38.3 wt % oil, 16.4 wt % PP, and 7.0 wt % peroxide based vulcanization recipe. The distribution function is obtained by the analysis of the T_2 decays measured using the DQ filtered HEPS experiment at different excitation time, t_{ex} (Figure 17b,c). The initial amplitude of the DQ filtered T_2 decays is normalized to the initial amplitude $A(0)^r$ of the T_2^r relaxation component (see eq 2). $A(0)^r$ is determined by the analysis of the HEPS data measured without the DQ filter. Only 18.5% of the magnetization of the rubbery phase is selected by the DQ filtered HEPS at the excitation time corresponding to the maximum of the DQ build up curve for EPDM (see Figure 16b). Since T_2 relaxation time for EPDM rubbers at temperatures above 90 °C is proportional to the weight-average molar mass of network chains (see eqs 4 and 5),[21] the T_2^r distribution might be related to the molar mass distribution of network chains in the EPDM phase of the TPV (see part 3.7).

4. Conclusions

The present study had the following objectives: (1) to establish a NMR T_2 relaxation method for selective characterization of different phases in EPDM/PP TPVs; (2) to determine the effect of TPV composition on molecular mobility in different phases/fractions and the network density in the rubbery phase of the TPVs; (3) to reveal the effect of molecular parameters, as determined in the present study, on some mechanical properties of the TPVs; (4) to establish new NMR methods for improving the selectivity of the T_2 relaxation analysis to different phases in complex polymeric materials and to characterize the dynamic heterogeneity in polymeric materials and rubbery networks.

(1) The proton NMR T_2 relaxation experiments, which were applied in the present study, open new possibilities for selective characterization of molecular mobility in different phases of TPVs, of network density in the rubbery phase of EPDM/PP TPVs and of the molecular heterogeneity of different phases. It is shown that the largest contrast in molecular mobility in the different phases/fractions of the TPVs is observed at 110 °C. At this temperature, the NMR relaxation method allows to perform a rather accurate determination of the phase composition and molecular mobility in the crystalline phase of PP, amorphous PP, EPDM, and oil. The reliability of the method for selective characterization of the TPV phases is proven by the fact that the sample composition, as determined by the T_2 analysis, is in

a good agreement with the composition used for the sample preparation.

(2) The NMR characterization of a series of TPV samples with a wide range of the compositions allows to establish several relationships between sample composition, molecular mobility, the network density in the rubbery phase, and some mechanical properties. The rubbery phase of the TPVs is mainly composed of EPDM and extender oil. The molar mass of EPDM network chains is determined by this method. The total network density in vulcanized oil-extended EPDM and TPVs with the same amount of PP decreases with increasing amount of oil due to a decrease in the entanglement density. Apparent chain entanglements are hardly present in EPDM at high concentrations of extender oil. The decrease in the entanglement density upon increasing oil content can be estimated using scaling approaches. Results of the present study suggest that propylene-rich chain fragments of EPDM and the amorphous PP phase form a thin interfacial layer, which is the source of physical junctions/entanglements at the EPDM/PP interface at the shell of the rubber particles and PP particles occluded in the EPDM phase. It is shown that the network density, $1/2M_{c+p+en}$, in the rubbery phase of TPVs is composed of chemical cross-links (c), chain entanglements between EPDM chains (en), and physical junctions (p) at the EPDM/PP interface. The total network density in the rubbery phase is affected by the following changes in the TPV composition: the network density increases with increasing amount of the cross-linker (phenolic resin) per weight unit of EPDM. $1/2M_{c+p+en}$ decreases with increasing oil content because of chain disentanglements. $1/2M_{c+p+en}$ increases with increasing PP/EPDM weight ratio due to an increase in the density of physical junctions at the EPDM/PP interface. A good correlation is observed between the network density in the rubbery phase of TPVs and the "cross-linking" parameter, which is defined by the following weight ratio: [PP × (phenolic resin)]/oil. The EPDM network density largely influences the translational and rotational mobilities of oil molecules: the higher the cross-link density, the more the mobility of oil molecules is hindered. A small fraction of oil molecules is mixed with the amorphous phase of PP causing plastization of the PP phase. The plastization effect increases with increasing weight ratio of oil/PP. Crystallinity of PP, as determined by the NMR method, is hardly affected by the TPVs composition and is close to 70 wt %.

(3) The phase composition, the network density in the rubbery phase and molecular mobility in different microphases of TPVs are discussed in relation to some mechanical properties. It is shown that the modulus of TPVs is largely determined by the amount of PP. The network density in the rubbery phase of TPVs has a moderate effect on the modulus. Both compression and tensile sets increase with an increase of PP content. An increase in the network density and the oil content improves the elastic recovery after compression and tension at short recovery time, both recovery after compression and tensile recovery.

(4) Two NMR methods are evaluated to improve the selectivity of the T_2 relaxation analysis to different phases of TPV. The methods are based on the inversion−recovery experiment and double-quantum (DQ) filtering of the decay of the transverse magnetization relaxation. It is shown that DQ filtering of T_2 relaxation experiments largely improves the selectivity of the NMR method to different phases in complex polymeric materials and could offer new possibilities for characterization of network heterogeneity.

Acknowledgment. Many thanks go to Maria Soliman for providing the TPV samples, their mechanical properties and for discussions. The author would like to thank Martin van Duin for discussions on an early stage of this study; Francesca Romana de Risi and Christian Hedesiu for assistance in performing the NMR T_2 relaxation experiments with the DQ filter, Dan Demco for discussion of results of the DQ experiments, and Jacques Noordermeer, Dan Demco, and Kay Saalwächter for comments on the manuscript.

References and Notes

(1) Legge, N. R.; Holden, G.; Schreoder, H. E. *Thermoplastic Elastomers*; Hanser Publishers: New York, 1987.
(2) Gergen, W. P.; Lutz, R.; Davidson, S. *Thermoplastic Elastomers: A Comprehensive Review*; Legge, N. R., Ed.; Carl Hanser, Munich, Germany, 1987.
(3) De, S. K.; Bhowmick, A. K. *Thermoplastic Elastomers from Rubber—Plastic Blends*; Ellis, Horwood Limited: Chichester, West Sussex, U.K., 1990.
(4) Coran, A. Y.; Patel, P. *Rubber Chem. Technol.* **1980**, *53*, 141.
(5) Sengupta, P.; Noordermeer, J. W. M. *Macromol. Rapid Commun.* **2005**, *26*, 542.
(6) Sengupta, P. Morphology of Olefinic Thermoplastic Elastomer Blends. Ph.D. Thesis, University of Twente, Enschede, The Netherlands, 2004.
(7) Yang, Y.; Chiba, T.; Saito, H.; Inoue, T. *Polymer* **1998**, *39*, 3365.
(8) Kikuchi, Y.; Fukui, T.; Okada, T.; Inoue, T. *J. Appl. Polym. Sci.: Appl. Polym. Symp.* **1992**, *50*, 261.
(9) Kawabata, S.; Kitawaki, S.; Arisawa, H.; Yamashita, Y.; Guo, X. *J. Appl. Polym. Sci.: Appl. Polym. Symp.* **1992**, *50*, 245.
(10) Ohlsson, B.; Hassander, H.; Tornell, B. *Polym. Eng. Sci.* **1996**, *36*, 501.
(11) Vennemann, N.; Hundorf, J.; Kummerlowe, C.; Schulz, P. *Kautschuk Gummi Kunstst.* **2001**, *54*, 362.
(12) Ellul, M. D. *Rubber Chem. Technol.* **1998**, *71*, 244.
(13) Litvinov, V. M. In *Spectroscopy of Rubbers and Rubbery Materials*; Litvinov, V. M.; De, P. P.; Eds.; RAPRA Technology: Shawbury, U.K., 2002; p 353 and references therein.
(14) Sengers, W. G. F.; Wübbenhorst, M.; Picken, S. J.; Gotsis, A. D. *Polymer* **2005**, *46*, 6391.
(15) Jayaraman, K.; Kolli, V. G.; Kang, S. Y.; Kumar, S.; Ellul, M. D. *J. Appl. Polym. Sci.* **2004**, *93*, 113.
(16) Winters, R.; Lughtenburg, J.; Litvinov, V. M.; van Duin, M.; de Groot, H. J. M. *Polymer* **2001**, *42*, 9745.
(17) Ellul, M. D.; Tsou, A. H.; Hu, W. *Polymer* **2004**, *45*, 3351.
(18) Marinovic, T.; Susteric, Z.; Dimitrievski, I.; Kranj, A.; Veksli, A.; *Kautschuk Gummi Kunstst.* **1998**, *51*, 189.
(19) Aluas, M.; Filip, C. *Solid State Nucl. Magn. Reson.* **2005**, *27*, 165.
(20) Litvinov, V. M.; Soliman, M. *Polymer* **2005** *46*, 3077.
(21) Litvinov, V. M.; Barendswaard, W.; van Duin, M. *Rubber Chem. Technol.* **1998**, *71*, 105.
(22) Orza, R. A.; Magusin, P. C. M. M.; Litvinov, V. M.; van Duin, M.; Michels, M. A. J. *Macromol. Symp.* **2005**, *230*, 144.
(23) Steenbrink, A. C.; Litvinov, V. M.; Gaymans, R. J. *Polymer* **1998**, *39*, 4817.
(24) van Duin, M. *Rubber Chem. Technol.* **1995**, *68*, 717.
(25) de Risi, F. R.; Litvinov, V. M.; Noordermeer, J. W. M. Manuscript in preparation.
(26) Litvinov, V. M.; Penning, J. P. *Macromol. Chem. Phys.* **2004**, *205*, 1721 and references therein.
(27) Kimmich, R. *NMR—Tomography, Diffusiometry, Relaxometry*; Springer-Verlag: Berlin, 1997.
(28) Spiess, H. W. *Colloid Polym. Sci.* **1983**, *261*, 193.
(29) Bilski, P.; Sergeev, N. A.; Wasicki, J. *Mol. Phys. Rep.* **2000**, *29*, 55.
(30) Bilski, P.; Sergeev, N. A.; Wasicki, J. *Mol. Phys.* **2003**, *101*, 335.
(31) Munowitz, M.; Pines, A. *Advances in Chemical Physics: Principles and Applications of Multiple-Quantum NMR*; Wiley-Interscience: New York 1987; Vol. 66, p 1.
(32) Saalwächter, K.; Ziegler, P.; Spyckerelle, O.; Haidar, B.; Vidal, A.; Sommer, J.-U. *J. Chem. Phys.* **2003**, *119*, 3468.
(33) Ba, Y.; Ripmesster, J. A. *J. Chem. Phys.* **1998**, *108*, 8589.
(34) Buda, A.; Demco, D. E.; Bertmer, M.; Blümich, B.; Litvinov, V. M.; Penning, J.-P. *J. Phys. Chem. B* **2003**, *107*, 5357.
(35) Buda, A.; Demco, D. E.; Bertmer, M.; Blümich, B.; Reining, B.; Keul, H.; Höcker, H. *Solid State Nucl. Magn. Reson.* **2003**, *24*, 39.
(36) Buda, A.; Demco, D. E.; Blümich, B.; Litvinov, V. M.; Penning, J.-P. *ChemPhysChem* **2004**, *5*, 876.
(37) Cherry, B. R.; Fujimoto, C. H.; Cornelius, C. J.; Alam, T. M. *Macromolecules* **2005**, *38*, 1201−1206.
(38) Hedesiu, C.; Kleppinger, R.; Demco, D. E.; Adams Buda, A.; Blümich, B.; Remerie, K.; Litvinov, V. M. *Polymer*, submitted.

CDV

(39) Fedotov, V. D.; Schneider, H. In *Structure and Dynamics Bulk Polymers by NMR Methods. NMR Basic Principles and Progress*; Diehl, P., Fluck, E., Gunter, H., Kosfeld, R., Seelig, I., Eds.; Springer: Berlin, 1989.
(40) McBrierty, V. J.; Packer, K. J. *Nuclear Magnetic Resonance in Solid Polymers*; Cambridge University Press: Cambridge, U.K., 1993.
(41) Kenwright, A. M.; Say, B. J. In *NMR Spectroscopy of Polymers*; Ibbett, R. N., Ed.; Blackie Academic & Professional: London, 1993; p 231.
(42) Tanaka, H.; Inoue, Y. *Polym. Int.* **1993**, *31*, 9.
(43) Dadauli, D.; Harris, R. K.; Kenwright, A. M.; Say, B. J.; Sünnetçioglu, M. M. *Polymer* **1994**, *35*, 4083.
(44) Dujourdy, L.; Bazile, J. P.; Cohen-Addad, J. P. *Polym. Int.* **1999**, *48*, 558.
(45) Schreurs, S.; François, J. P.; Adriaensens, P.; Gelan, J. *J. Phys. Chem.* **1999**, *103*, 1393.
(46) Weglarz, W. P.; Peemoeller, H.; Rudin, A. *J. Polym. Sci., Part B: Polym. Phys.* **2000**, *38*, 2487.
(47) Hansen, E. W.; Kristiansen, P. E.; Pedersen, B. *J. Phys. Chem. B* **1998**, *102*, 5444.
(48) Kristiansen, P. E.; Hansen, E. W.; Pedersen, B. *J. Phys. Chem. B* **1999**, *103*, 3552.
(49) Cohen-Addad, J. P. *Prog. NMR Spectrosc.* **1993**, *25*, 1.
(50) Cohen-Addad, J. P. In *Spectroscopy of Rubbery Materials;* Litvinov, V. M.; De, P. P.; Eds.; RAPRA Technology: Shawbury, U.K., 2002; p 291.
(51) Brereton, M. G. *Macromolecules* **1990**, *23*, 1119.
(52) Brereton, M. G. *Macromolecules* **1991**, *24*, 2068.
(53) Cohen-Addad, J. P.; Girard, O. *Macromolecules* **1992**, *25*, 593.
(54) Kulagina, T. P.; Litvinov, V. M.; Summanen, K. T. *J. Polym. Sci., Part B: Polym. Phys.* **1993**, *31*, 241.
(55) Cohen-Addad, J. P.; Dupeyre, R. *Polymer* **1983**, *24*, 400.
(56) Saalwächter, K.; Heuer, A. *Macromolecules* **2006**, *39*, 3291.
(57) Ries, M. E.; Klein, P. G.; Brereton, M. G.; Ward, I. M. *Macromolecules* **1998**, *31*, 4950.
(58) Kimmich, R.; Köpf, M.; Callaghan, P. *J. Polym. Sci., Part B: Polym. Phys.* **1991**, *29*, 1025.
(59) Gotlib, Y. Y.; Lifshits, M. I.; Shevelev, V. A.; Lishanskii, I. A.; Balanina, I. V. *Polym. Sci. USSR* **1976**, *18*, 2630.
(60) Fry, C. G.; Lind, A. C. *Macromolecules* **1988**, *21*, 1292.
(61) Richter, D.; Farago, B.; Butera, R.; Fetters, L. J.; Huang, J. S.; Ewen, B. *Macromolecules* **1993**, *26*, 795 and references therein.
(62) Orza, R. A.; Magusin, P. C. M. M.; Litvinov, V. M.; van Duin, M.; Michels, M. A. J. *Macromol. Symp.* **2005**, *230*, 144.
(63) Litvinov, V. M.; Dias, A. A. *Macromolecules* **2001**, *34*, 4051.
(64) Saalwächter, K. *Macromolecules* **2005**, *38*, 1508.
(65) Saalwächter, K.; Herrero, B.; López-Manchado, M. A. *Macromolecules* **2005**, *38*, 4040.
(66) Saalwächter, K.; Klüppel, M.; Luo, H.; Schneider, H. *Appl. Magn. Reson.* **2004**, *27*, 401.
(67) Anderson, S. L.; Grulke, E. A.; DeLassus, P. T.; Smith, P. B.; Kocher, C. W.; Landes, B. G. *Macromolecules* **1995**, *28*, 2944.
(68) Valiæ, S.; Sotta, P.; Deloche, B. *Polymer* **1999**, *40*, 989.
(69) Valiæ, S.; Judeinstein, P.; Deloche, B. *Polymer* **2003**, *44*, 5263.
(70) Deloche, B.; Sotta, P. In *Spectroscopy of Rubbers and Rubbery Materials*; Litvinov, V. M., De, P. P., Eds.; RAPRA Technology: Shawbury, U.K., 2002; p 557.
(71) De Gennes, P. G. *Scaling Concepts In Polymer Physics*; Cornell University Press: Ithaca, NY, 1979.
(72) Iwata, K.; Edwards, S. F. *J. Chem. Phys.* **1989**, *90*, 4567.
(73) Kavassalis, T. A.; Noolandi, J. *Macromolecules* **1989**, *22*, 2709.
(74) Colby, R. H.; Fetters, L. J.; Funk, W. F.; Graessley, W. W. *Macromolecules* **1991**, *24*, 3873.
(75) Colby, R. H.; Rubinstein, M.; Viovy, J. L. *Macromolecules* **1992**, *25*, 996.
(76) Richter, D.; Farago, B.; Butara, R.; Fetters, L. J.; Huang, J. S.; Ewen, B. *Macromolecules* **1993**, *26*, 795.
(77) Tao, H.; Huang, C.-I.; Lodge, T. P. *Macromolecules* **1999**, *32*, 1212.
(78) Westermann, S.; Willner, L.; Richter, D.; Fetters, L. J. *Macromol. Chem. Phys.* **2000**, *201*, 500.
(79) Chen, Z.; Cohen, C.; Escobedo, F. A. *Macromolecules* **2002**, *35*, 3296.
(80) Litvinov, V. M.; Steeman, P. A. M. *Macromolecules* **1999**, *32*, 8476.
(81) Litvinov, V. M.; Braam, A. W. M.; van der Ploeg, A. F. M. J. *Macromolecules* **2001**, *34*, 489.
(82) Litvinov, V. M. *Macromolecules* **2001**, *34*, 8468.
(83) Wouters, M. E. L.; Litvinov, V. M.; Binsbergen, F. L.; Goossens, J. P. G.; van Duin, M.; Dikland, H. G. *Macromolecules* **2003**, *36*, 1147.
(84) Stern, S. A.; Trohalaki, S. In *Barrier Polymers and Structures*, Koros, W. J., Ed.; ACS Symposium Series 423; American Chemical Society: Washington, DC, 1990; p 22.
(85) Sotta, P.; Deloche, B. *Macromolecules* **1990**, *23*, 1999. Sotta, P. *Macromolecules* **1998**, *31*, 8417.
(86) Lienin, S. F.; Brüschweiler, R.; Ernst, R. R. *J. Magn. Reson.* **1998**, *131*, 184.
(87) Graf, R.; Demco, D. E.; Hafner, S.; Spiess, H. W. *J. Chem. Phys.* **1997**, *106*, 885.
(88) Schneider, M.; Gasper, L.; Demco, D. E.; Blümich, B. *J. Chem. Phys.* **1999**, *111*, 402.
(89) Graf, R.; Demco, D. E.; Hafner, S.; Spiess, H. W. *Solid State Nucl. Magn. Reson.* **1998**, *12*, 139.
(90) Fechete, R.; Demco, D. E.; Blümich, B. *J. Magn. Reson.* **2004**, *169*, 19.
(91) Saalwächter, K.; Kleinschmidt, F.; Sommer, J.-U. *Macromolecules* **2004**, *37*, 8556.
(92) Voda, M. A.; Demco, D. E.; Perlo, J.; Orza, R. A.; Blümich, B. *J. Magn. Reson.* **2005**, *172*, 98.
(93) Saalwächter, K.; Herrero, B.; López-Manchado, M. A. *Macromolecules* **2005**, *38*, 9650.
(94) Wang, M.; Bertmer, M.; Demco, D. E.; Blümich, B.; Litvinov, V. M.; Barthel, H. *Macromolecules* **2003**, *36*, 4411.
(95) Bertmer, M.; Gasper, L.; Demco, D. E.; Blümich, B.; Litvinov, V. M. *Macromol. Chem. Phys.* **2004**, *205*, 83.

MA061911H